

THESIS FOR THE DEGREE OF DOCTOR OF PHILOSOPHY

in

Machine and Vehicle Systems

# Muscle Responses of Car Occupants

Numerical Modeling and Volunteer Experiments under  
Pre-Crash Braking Conditions

JONAS ÖSTH



Division of Vehicle Safety  
Department of Applied Mechanics  
CHALMERS UNIVERSITY OF TECHNOLOGY  
Gothenburg, Sweden, 2014

**Muscle Responses of Car Occupants:  
Numerical Modeling and Volunteer Experiments under Pre-Crash Braking Conditions**

JONAS ÖSTH

ISBN 978-91-7385-987-5

© JONAS ÖSTH, 2014.

Doktorsavhandlingar vid Chalmers tekniska högskola  
Ny serie nr 3668  
ISSN 0346-718X

Division of Vehicle Safety  
Department of Applied Mechanics  
Chalmers University of Technology  
SE-412 96 Gothenburg  
Sweden  
Telephone + 46 (0)31-772 1000

Cover:

Finite element human body model equipped with feedback controlled muscles in a simulated maximum driver braking event, see Section 5.5. Image by Jonas Östh.

Printed by Chalmers Reproservice  
Gothenburg, Sweden, 2014

# Muscle Responses of Car Occupants: Numerical Modeling and Volunteer Experiments under Pre-Crash Braking Conditions

JONAS ÖSTH

Division of Vehicle Safety

Department of Applied Mechanics

Chalmers University of Technology

## **Abstract**

Over 30 000 fatalities related to the road transport system are reported annually in Europe. Of these fatalities, the largest share is car occupants, even though significant improvements in vehicle safety have been achieved by the implementation of in-crash restraints and pre-crash driver support systems. Integration of pre-crash and in-crash safety systems has a potential to further reduce car occupant fatalities and to mitigate injuries. The aims of this thesis are to study the muscle responses of car occupants subjected to integrated safety interventions, and to model them in a numerical human model with active muscles. More specifically, pre-crash braking with standard and reversible pre-tensioned restraints is investigated.

A method to model car occupant muscle responses in a finite element (FE) human body model (HBM) was developed, utilizing feedback control of Hill-type muscle elements. It was found that the car occupant response to autonomous braking can be modeled with feedback control, by which stabilizing muscle activations are generated in response to external perturbations. However, modeling driver initiated braking requires the inclusion of a hypothesized anticipatory feed-forward response. Volunteer tests to provide validation data for the HBM were conducted, analyzed, and utilized for model validation. It was found that, in some car occupants, seat belt pre-tension can cause a startle response in the form of a bilateral, simultaneous, short peak contraction of all upper body muscles. Car occupant muscle activation levels during normal driving and in braking events were also quantified in percent of maximum voluntary efforts. The HBM developed with active muscles was able to capture the kinematic response of the volunteers in these events, with muscle activation levels of magnitude similar to that of the volunteers.

The method to model muscle responses with feedback control in an FE HBM has the potential to improve the model response in all pre-crash and in-crash scenarios in which muscle contraction can influence occupant kinematics, for instance multiple events and roll-over accidents. It provides a means for the virtual development of advanced integrated restraints that can lead to improved vehicle safety and a reduced number of fatalities and injuries in the road traffic environment.

**Keywords:** active muscle; occupant kinematics; feedback postural control; anticipatory postural control; human body model; finite element; autonomous braking; driver braking; electromyography; seat belt pre-tension

## List of Appended Publications

This thesis consists of the following six papers, referred to by Roman numerals.

- I. Östh J, Brolin K, Happee R (2012) Active Muscle Response using Feedback Control of a Finite Element Human Arm Model. *Computer Methods in Biomechanics and Biomedical Engineering* 15(4):347–361.
- II. Östh J, Brolin K, Carlsson S, Wismans J, Davidsson J (2012) The Occupant Response to Autonomous Braking: A Modeling Approach that Accounts for Active Musculature. *Traffic Injury Prevention* 13(3):265–277.
- III. Östh J, Ólafsdóttir JM, Davidsson J, Brolin K (2013) Driver Kinematic and Muscle Responses in Braking Events with Standard and Reversible Pre-tensioned Restraints: Validation Data for Human Models. *Stapp Car Crash Journal* 57:1–41.
- IV. Ólafsdóttir JM, Östh JKH, Davidsson J, Brolin K (2013) Passenger Kinematics and Muscle Responses in Autonomous Braking Events with Standard and Reversible Pre-tensioned Restraints. *Proceedings of the IRCOBI Conference*; Gothenburg, Sweden, pp. 602–617.
- V. Östh J, Brolin K, Bråse D (2014) A Human Body Model with Active Muscles for Simulation of Pre-Tensioned Restraints in Autonomous Braking Interventions. Submitted for publication.
- VI. Östh J, Eliasson E, Happee R, Brolin K (2014) A Method to Model Anticipatory Postural Control in Driver Braking Events. Manuscript.

## **Division of Work**

- I. The concept for the paper was developed by Jonas Östh and Karin Brolin, model implementation and simulation were done by Jonas Östh with the advice of Karin Brolin and Riender Happee, and volunteer experiments were conducted at the initiative of Riender Happee. Jonas Östh wrote the manuscript.
- II. Jonas Östh planned the study with support from Karin Brolin, Johan Davidsson, and Jac Wismans. The validation data was taken from a study conducted by Stina Carlsson and Johan Davidsson, who assisted Jonas Östh in further analysis of the data. Jonas Östh wrote the manuscript.
- III. The study was planned by Jonas Östh jointly with Johan Davidsson and Karin Brolin, while the test setup was developed by Jonas Östh and Johan Davidsson. Jonas Östh and Jóna Marín Ólafsdóttir conducted the experiments, while Jonas Östh did most of the data analysis with support from Jóna Marín Ólafsdóttir. The manuscript was written by Jonas Östh.
- IV. The study was planned by Jonas Östh jointly with Johan Davidsson and Karin Brolin, while the test setup was developed by Jonas Östh and Johan Davidsson. Jonas Östh and Jóna Marín Ólafsdóttir conducted the experiments, while Jóna Marín Ólafsdóttir did most of the data analysis with support from Jonas Östh. The manuscript was written by Jóna Marín Ólafsdóttir.
- V. Jonas Östh planned the study, developed the model, conducted the simulations and analyzed the data. Furthermore, Jonas Östh made the parameter study with the advice of Dan Bråse, who also assisted in the development of the test vehicle instrumentation used to generate the volunteer data. Jonas Östh wrote the manuscript.
- VI. Jonas Östh came up with the idea for the paper based on discussions with Riender Happee and Karin Brolin. Erik Eliasson implemented the lower extremity musculoskeletal model. Jonas Östh implemented the anticipatory postural control, and carried out all simulations and data analysis. Jonas Östh wrote the paper.

## **Preface**

The work presented in this thesis was carried out at Chalmers University of Technology, at the Division of Vehicle Safety, in the Injury Prevention Research group from 2009–2014, under the supervision of Associate Professor Karin Brolin, Associate Professor Johan Davidsson, and Professor Jac Wismans.

From 2009–2011 the research was funded by SAFER, the Vehicle and Traffic Safety Centre at Chalmers, and from 2012–2014 by VINNOVA, the Swedish Governmental Agency for Innovation Systems, as part of the FFI Vehicle and Traffic Safety research programme. Project partners were Autoliv Research AB, Volvo Car Corporation, Volvo Group, SAAB Automobile, and Umeå University.

The research was conducted at the SAFER office in Gothenburg. Many of the simulations were carried out with resources provided by the Swedish National Infrastructure for Computing (SNIC) at C3SE.

## **Acknowledgements**

I am grateful to many people, for supporting me in my endeavor as a Ph.D. student, and I would like to thank:

My supervisors Karin Brolin, Johan Davidsson, and Jac Wismans for providing me with valuable advice and inspiration; Riender Happee at Delft University of Technology for fruitful cooperation and supervision at the beginning and end of my Ph.D. studies; the industrial partner group consisting of Bengt Pipkorn, Autoliv Research AB, Lotta Jakobsson and Merete Östman, Volvo Car Corporation, Fredrik Törnvall, Fredrik Jenefelt, and Stefan Thorn, Volvo Group, and Mats Lindqvist, SAAB Automobile and Umeå University.

Moreover, I am thankful to: My former colleague at Volvo Car Corporation, Bart de Korte, for helping me with information about the brake performance of our test vehicles; Dan Bråse at Autoliv Research AB for expert help with instrumenting our test vehicle; Johan Svensson and Anders Axelsson at Volvo Car Corporation for help with the test vehicle; Göran Stigler, Chalmers, for help with the design and manufacturing of electronic test equipment; Björn Äng, Karolinska Institutet, for excellent help with electromyography methods; and all of the volunteers who participated in our tests.

I also wish to thank: Thomas Borrvall, Dynamore Nordic AB, for getting me started with Fortran, the LS-DYNA user subroutine, and MPI programming; Jimmy Forsberg, Dynamore Nordic AB, for support with LS-OPT; Susumu Ejima at Japan Automotive Research Institute, for providing plot data and clarifying information regarding human volunteer tests used for model development; Niklas Höglund, Volvo Car Corporation, for the seat model; and Lora Sharp McQueen for the language editing of this thesis and all appended publications of which I am the main author.

It was inspiring to supervise the work of my M.Sc. students, Hamid Khodaei, Salar Mostofizadeh, and Samuel Andersson. I am grateful to: B.Sc. students Niklas Blomgren, Erik Eliasson, Joakim Ericsson, and Oscar Lundahl, for help with the lower extremity model; my colleagues at the SAFER office who have provided not only a stimulating work environment, but also a lot of valuable professional help.

Special thanks go to my family: My sister, Jenny, for inspiring me to pursue a career in engineering; my brother, Jan, my mother, Karin, and father, Tommy for always supporting me and my family; my wife, Katarina, for her constant love and support, and my children, Joakim and Selma, for providing me with a meaning for all efforts spent at work.

## **Acronyms**

Active HBM – A Human Body Model with actively controlled muscles  
AHBM – The Active Human Body Model developed as part of this thesis work  
ATD – Anthropomorphic Test Device  
CE – Contractile Element  
CNS – Central Nervous System  
EMG – Electromyography  
EU27 – The 27 European Union member states prior to 2013  
FE – Finite Element  
g – Gravitational acceleration at the surface of the Earth, approx.  $9.81 \text{ m/s}^2$   
HBM – Human Body Model  
Hybrid III – Frontal impact anthropomorphic test device  
MB – Multibody  
MVC – Maximum Voluntary Contraction  
PE – Parallel Elastic element  
PID – Proportional, Integral, and Derivative  
PMHS – Post Mortem Human Subject  
PNS – Peripheral Nervous System  
SE – Series Elastic element  
THOR – Frontal impact anthropomorphic test device  
THUMS – Total Human Model for Safety (Toyota 2008)  
TNO – The Netherlands Organization for Applied Scientific Research  
USA – The United States of America  
1D – One Dimensional  
3D – Three Dimensional

## Table of Contents

Abstract.....	iii
List of Appended Publications.....	iv
Division of Work.....	v
Preface.....	vi
Acknowledgements .....	vii
Acronyms.....	viii
1 Introduction .....	1
1.1 Numerical Human Body Models .....	2
1.2 Integrated Safety Systems.....	3
1.3 Aims.....	4
2 Biomechanics of the Neuromuscular System.....	5
2.1 Skeletal Muscles.....	5
2.2 The Nervous System.....	8
2.3 Motor Control .....	9
3 Review of Active Muscle Control in HBMs .....	13
3.1 Open-loop Muscle Activation .....	16
3.1.1 Reflex Activation.....	16
3.1.2 Optimization of Static Posture-Maintaining Activations .....	16
3.1.3 Optimization of Dynamic Activations .....	17
3.1.4 Estimation based on Experimental Data.....	17
3.2 Closed-loop Muscle Activation.....	17
3.2.1 Torque Actuators .....	18
3.2.2 Line Muscle Elements.....	18
4 Review of Volunteer Tests of Muscle Responses .....	21
4.1 Frontal Impacts and Braking Scenarios .....	21
4.2 Lateral Impacts and Vehicle Maneuvers .....	22
4.3 Rear-End Impacts.....	22
4.4 Driving Simulators.....	23

5	Summaries of Appended Papers .....	25
5.1	Paper I .....	25
5.2	Paper II.....	26
5.3	Papers III and IV .....	27
5.4	Paper V.....	28
5.5	Paper VI.....	29
6	Discussion.....	31
6.1	Model Development.....	31
6.1.1	Postural Feedback Control in Finite Element HBMs.....	32
6.1.2	Validation and Application.....	33
6.2	Car Occupant Muscle Responses.....	34
6.2.1	Autonomous Braking and Light Impacts .....	34
6.2.2	Driver Voluntary Braking .....	35
6.2.3	Variations in Occupant Postural Responses .....	36
6.3	Limitations and Future Work.....	37
7	Conclusions .....	39
8	References.....	41
	Appendix A: Implementation of the AHBM.....	51
A.1	Notation .....	51
A.2	Musculoskeletal Model .....	52
A.3	Controller Model .....	54
A.4	Muscle Recruitment and Activation Dynamics .....	56
A.5	Muscles Included.....	57
A.6	References .....	63

## 1 Introduction

In the year 2010, there were 319 fatalities related to the road transport system reported in Sweden (European Commission 2012). For the 27 European Union member states (EU27) the number of fatalities was 31 000 (European Commission 2012) and for the United States of America (USA) the figure was 29 800 (NHTSA 2012). In addition, 23 300, 1 500 000 (European Commission 2013), and 2 217 000 (NHTSA 2012) injuries were reported for each these regions, respectively. While these figures are unacceptably high, the fatalities are only 34%, 41%, and 64% of the number of fatalities for each of the regions reported in 1990, even though the distances travelled have increased by approximately 15% and 40% in Sweden and the USA, respectively, over the same period of time, and by 21% in the EU27 between 1995 and 2010. Hence, road traffic safety is improving in the developed world.

Large contributions to the improvement of vehicle safety since the 1950s can be attributed to in-crash systems such as improved vehicle structures and occupant restraints, in particular the three-point seat belt which was first introduced in 1957. Early studies showed an injury reduction potential of 40–90% (Bohlin 1967) or more than 35% (Norin *et al.* 1984). Cummings *et al.* (2003) estimated a 61% lower risk of death, using accident data from 1986–1998, for front seat occupants wearing a seat belt compared with unbelted occupants.

More recently, accident avoidance and pre-crash systems that avoid or mitigate the severity of accidents have been implemented on a large scale. The most important system to date is probably vehicle stability control, which was introduced in a mass market car model in 1998. By 2010, in Sweden, 99% of all new cars were equipped with it (Lie *et al.* 2013). Vehicle stability control provides driver assistance in critical driving situations, and has been shown to reduce the occurrence of fatal, and serious loss of control, accidents on low-friction surfaces by 50%, and by at least 13% for all types of crashes (Lie *et al.* 2006).

Vehicle stability control is implemented by individual wheel braking using sensory information about the vehicle state. With the same hardware, combined with additional information from a radar sensor, autonomous braking systems have been introduced (Coelingh *et al.* 2007; Schittenhelm 2009), with the potential to mitigate the severity of or to avoid rear end collisions. As more information about the state of the vehicles and the surroundings of the vehicle becomes available, for instance through vehicle-to-vehicle communication, it becomes possible to predict upcoming accidents. Therefore, in emerging integrated safety systems, measures to reposition or restrain the vehicle occupants can be taken before an impact has commenced. An example of such a system is PRE-SAFE (Schöneburg *et al.* 2011), which uses reversible seat belt pre-tension, to remove belt slack and secure the occupant, in combination with autonomous braking prior to an impact.

Although the fatalities and injuries summarized above consist of multiple groups of road users, *e.g.* pedestrians or bicyclists, the largest group is car occupants, who accounted for approximately 70% of the road fatalities in Sweden in 2009 (European Commission 2012) and for 50% of the EU road fatalities in 2010 (WHO 2013). Even though large improvements in car occupant safety have been made, there is still an urgent need for greater safety.

## **1.1 Numerical Human Body Models**

With increasing computational power available, numerical simulation has become an important tool for all types of product development, especially in the automotive industry. To evaluate the risk of injury in a simulated vehicle crash, models of the occupants are needed. In physical testing this task is performed by mechanical models of the human, anthropomorphic test devices (ATD), commonly known as crash test dummies. Numerical models of ATD exist and are used extensively (Prasad and Chou 2002), but more detailed responses can be evaluated if the occupants are represented by a human body model (HBM).

An HBM is a numerical anthropomorphic model of the human body or a part of the human body. In principle, two modeling approaches are utilized: a multi-body systems (MB) method, by which the human body is approximated with a system of flexible and rigid bodies connected by kinematic joints, and the finite element (FE) method by which the anatomical structures are divided into smaller elements, defined by nodal points, for which approximate solutions to the governing differential equations are determined. The MB method has the advantage of requiring shorter computational time due to less complex models, while the FE method facilitates the study of injury risk at tissue level and is better suited for contact simulation. However, it is common that HBMs are hybrid models that utilize both types of modeling approaches.

Wismans *et al.* (1979) proposed an early whole body pediatric HBM, consisting of nine rigid bodies connected by eight kinematic joints, and concluded that the HBM was better than a pediatric ATD to represent the kinematics of a cadaveric subject in a 20 g sled test. The pediatric HBM was modeled in the MB software MADYMO (TASS 2013). The MADYMO software has been continuously developed, and is today commonly used for occupant modeling in automotive industry and research. A male 50<sup>th</sup> percentile whole body HBM, consisting of 24 rigid vertebrae, seven flexible bodies for the thorax and multi-part extremities, was presented by Happee *et al.* (1998).

The FE HBMs also originate from the 1970s when they were primarily models of specific body parts (Yang *et al.* 2006), in particular the head and brain (*e.g.* Shugar 1975; Ward and Thompson 1975). A few whole body FE HBMs exist today, *e.g.* the HUMOS (Robin 2001), the THUMS (Iwamoto *et al.* 2002) or the GHBMC model (Park *et al.* 2013). In both academic and automotive industry research, these HBMs are simulated using commercial explicit FE solvers, for instance Radioss (Altair 2013), PAM-CRASH (ESI 2013), or LS-DYNA (LSTC 2013).

A modern HBM such as the THUMS version 4 (Toyota 2011) has a high level of detail, with over 1.8 million finite elements to represent a 50<sup>th</sup> percentile male occupant. However, even such a complex model is still a simplification due to the complexity of the human anatomy and the mechanical properties of biological tissues. Therefore, in the development of HBMs many aspects have not yet been modeled in detail and remain to be investigated. In this thesis the focus is on the inclusion and control of muscles in HBMs, which is required for the simulation of events where the loading is limited to a few g and the duration is long enough to allow the neuromuscular system of car occupants time to react. Such events are typically associated with pre-crash actions and reactions of car occupants, *e.g.* emergency braking or steering.

## 1.2 Integrated Safety Systems

Commonly, vehicle safety systems are divided into to three main categories with a few different names. First, systems active prior to the accident are denoted pre-crash, primary, or active systems. Second, systems active during the crash are called in-crash, secondary, or passive systems. Third, systems that are active after the crash has taken place are denoted post-crash or tertiary systems. As mentioned previously, the boundary between these types of systems are becoming less distinct with the increasing sensory information, actuators, and processing power available in modern vehicles. In particular, the combination of pre-crash accident avoidance and in-crash protection is denoted as integrated safety (Seiffert and Gonter 2014). Aparicio (2005) identified five possible actions of present and predicted future integrated safety technologies: “*Decrease vehicle speed; Prepare the vehicle for impact; Prepare occupants for impact; Optimize impact angle; and Alert the driver*”. Some of these technologies involve interaction with the vehicle occupants. Hence, HBMs are also potential tools for evaluation of integrated safety systems.

Systems that decrease vehicle speed by autonomous braking have already been introduced (Coelingh *et al.* 2007; Distner *et al.* 2009; Schittenhelm 2009). It is clear that the effect of such systems is beneficial, as the kinetic energy of the vehicle before the accident is decreased by autonomous braking. However, Antona *et al.* (2010) noted that, for equivalent speed impacts, accident statistics indicated a higher incidence of chest injuries for drivers who performed an emergency braking prior to the impact. Therefore, they made a study with an FE HBM in which a 0.8 g brake pulse was applied prior to a 55 km/h impact, compared with no pre-impact braking. It was found that, with pre-crash braking, maximum chest deflection and seat belt force were increased, from 44 mm to 51 mm and 6000 N to 6700 N, because the model already had a forward motion prior to the impact. This indicated a higher risk of injury due to pre-crash deceleration at equivalent impact speeds, which may be possible to mitigate by the development of integrated restraint systems.

To improve restraint functionality, and prepare occupants for impact, reversible pre-tension systems have been introduced together with autonomous braking (Schöneburg *et al.* 2011); this allows the occupant to be more tightly coupled to the seat belt during the autonomous braking, which reduces the forward motion studied by Antona *et al.* (2010). Reversible seat belt pre-tension has also been studied in combination with driver emergency braking (Tobata *et al.* 2003), lateral maneuvers (Mages *et al.* 2011), pre-impact braking (Woitsch and Sinz 2014), sled tests (Ito *et al.* 2013), and stationary conditions (Good *et al.* 2008a; Good *et al.* 2008b; Develet *et al.* 2013). In these studies, volunteers or ATDs were used. However, ATDs have severe limitations: they are developed to predict injury in high energy impacts and are too stiff to represent relaxed vehicle occupants under low loading conditions (Beeman *et al.* 2012). The volunteers are the best option, but as volunteers cannot be subjected to an injurious load, it is not possible to study directly the injury reduction potential of pre-crash activated integrated safety systems using volunteers. Both ATD and volunteer testing are also time consuming and costly. Hence, there is a need for numerical HBMs that can represent occupant responses in pre-crash loading conditions (Schöneburg *et al.* 2011, Mages *et al.* 2011). Such an HBM could also allow for the simulation of events that are a combination of pre-crash and in-crash loading (*e.g.* Antona *et al.* 2010). This HBM needs to include active musculature and a human-like control strategy of the muscles; the passive HBM would resemble post mortem human subjects (PMHS) that, in contrast to the ATD, are too soft in comparison with relaxed volunteers (Beeman *et al.* 2012).

### **1.3 Aims**

The objective of this thesis work is to study the muscle responses of car occupants subjected to pre-crash braking scenarios, and to develop an active HBM (AHBM) that can be used for the virtual development of integrated safety systems in this type of scenario. Two parallel, symbiotic, approaches are employed for this purpose. A method to model car occupant muscle responses in an FE HBM was developed and volunteer tests of car occupants subjected to pre-crash braking were carried out. The AHBM was validated with respect to the volunteer data and applied to investigate postural control strategies in autonomous and driver braking.

## 2 Biomechanics of the Neuromuscular System

The human body has three main types of muscle tissue: skeletal muscles, heart muscles, and smooth muscles. Skeletal muscles are responsible for movement and maintenance of posture and are subject to both voluntary and autonomous control from the central nervous system (CNS).

### 2.1 Skeletal Muscles

Skeletal muscle consists of muscle fibers, each fiber being an individual cell that can have several nuclei along its length. The main part of the muscle fiber consists of a repeated pattern of sarcomeres, built up by two overlapping types of contractile proteins: actin and myosin. Upon activation of the muscle fiber, the actin and myosin chains attach to each other through cross-bridges. This process is responsible for the generation of active muscle contractile force at the microscopic level.

The muscle fibers are held together by sheets of connective tissue, see Figure 1: the endomysium surrounding the fiber, the perimysium that covers several fibers, and finally the epimysium that surrounds the entire muscle. At the ends of the muscle the connective tissue forms tendons that attach to the skeletal structures of the body.

**Structure of a Skeletal Muscle**

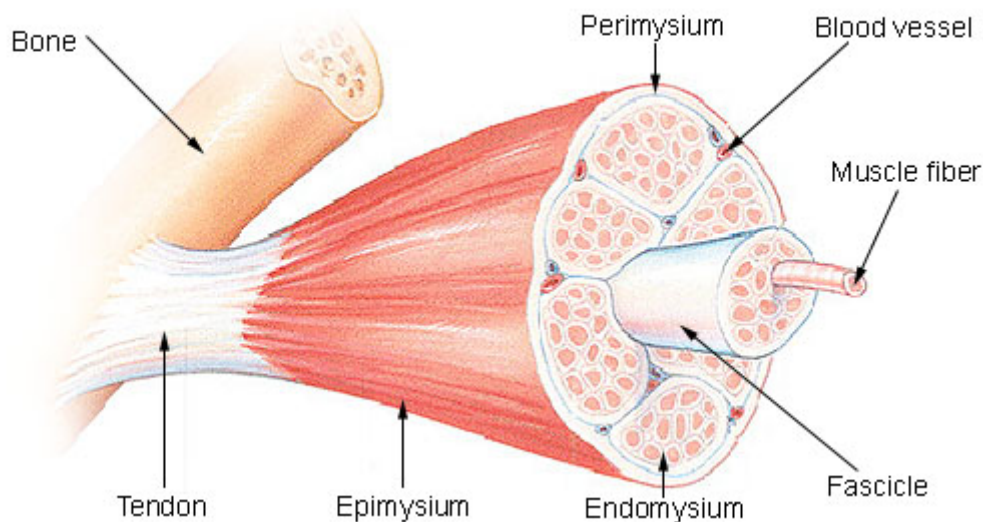


**Figure 1. The structure of skeletal muscles. Adapted from Wikimedia (2013).**

To model the mechanical properties of muscle tissue, two modeling approaches are common: detailed biophysical cross-bridge models (Huxley 1957) and phenomenological Hill-type models (Hill 1938; 1970; Winters and Stark 1985). The Hill-type models are more suitable than the cross-bridge ones to model transient events (van den Bogert *et al.* 1998), as they provide more accurate force responses in a wide range of conditions, and they also have the advantage of a lower complexity.

In a Hill-type model the mechanical properties of the muscle tissue are described by the three elements shown in Figure 2. The Parallel Elastic (PE) element represents the stiffness of the passive muscle tissue; the PE element is usually modeled with non-linear characteristics as shown in Figure 3. The PE element can also include a rate-dependent term, modeling the viscoelastic properties of the passive muscle tissue. The Series Elastic (SE) element can be regarded as the tendons by which the muscle is connected to the skeletal structure. Although the SE and PE elements have a similar shape for the force-length relation, the SE element is usually approximately ten times stiffer.

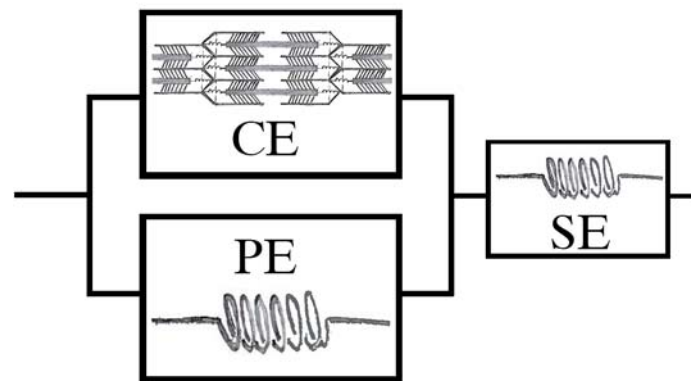


**Figure 2. Hill-type muscle model. CE = Contractile element; PE = Parallel elastic element; SE = Series elastic element.**

The Contractile Element (CE) generates an active force when the muscle is activated by nervous stimulation. Force produced by the CE is a function of the current activation level, muscle length, and shortening velocity. The length dependency of the CE can be seen in Figure 3(a), which shows that a maximum force is produced at a reference length,  $l_{opt}$ , with decreasing force for longer or shorter muscle length.

The force-velocity relation of the CE can be seen in Figure 3(b). For muscle shortening (concentric muscle contraction,  $V/V_{max} < 0$ ), the muscle force decreases until the maximum shortening velocity is reached. In the other direction ( $V/V_{max} > 0$ ), the muscle is forced to lengthen and is in eccentric contraction. During an eccentric contraction the muscle force increases with rising lengthening velocity above the maximum isometric force, which gives a dampening behavior to eccentrically stretched active muscle tissue.

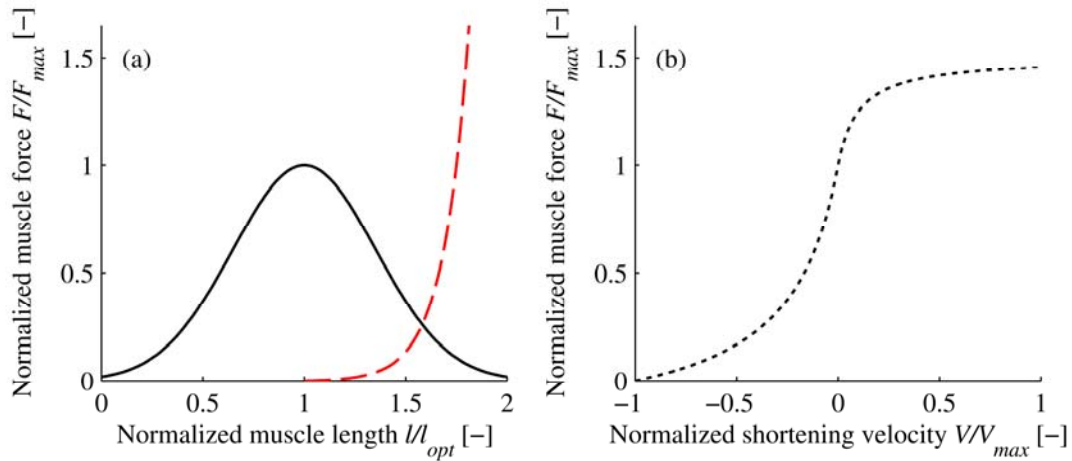


**Figure 3. Active muscle force-length (solid line), force-velocity (dotted line), and passive elastic force (dashed) relations in a Hill-type muscle model.**

The force-length and force-velocity properties of active muscle tissue are related to the forming and breaking of cross-bridges in the sarcomeres. At the reference length,  $l_{opt}$ , the maximal numbers of cross-bridges are available to form; for longer or shorter lengths the actin and myosin filament overlaps are reduced. As fewer cross-bridges can be formed, this leads to reduced contractile force. When the muscle is shortening, the cross-bridges must be broken and new ones formed. This process takes a finite amount of time; hence, tension cannot be sustained for increasing velocity. In eccentric contractions, muscle force increases, possibly due to the fact that breaking cross-bridges requires larger force than what is produced under isometric conditions (Winter 2009).

When using a Hill-type model, either experimental curves for the relations in Figure 3 can be used in the model, or approximating functions that fit the experimental data with shape factors. Approximation functions for the musculoskeletal model used in this thesis are described in detail in Paper I and in Appendix A.

In skeletal muscles, contraction is controlled by motor nerves that convey motor commands from the CNS to the muscles. The motor nerves consist of several neurons each of which attach to a motor unit, a group of muscle fibers that are recruited simultaneously by the neuron. Contraction commands to the muscles from the motor neurons are digital impulses; it is the frequency of the impulses that determines the level of contraction in each muscle fiber. The level of contraction of a whole muscle is also controlled by the number and size of the motor units that are being recruited.

When a contraction signal is received at the synaptic junction between the muscle fiber and the motor neuron, an action potential that spreads along the muscle fiber is generated. The action potential is a flux of ions through the cell membrane, and can be assessed experimentally as the electromyogram (EMG). Following the action potential, calcium ions are released inside the muscle fiber, and the presence of calcium ions allows the cross-bridges to form. Immediately after an action potential,

the cell membrane is restored, calcium levels are decreased, and muscle tension drops again. However, the deactivation process is slower than the activation process, and with increasing neural stimulation frequency a constant level of force will be achieved as the muscle fiber will not have time to relax. Thus, the muscle fibers act as low-pass filters for the discrete neural stimulation, and continuous muscle activation as a function of time is usually assumed in Hill-type muscle models.

## **2.2 The Nervous System**

The neurons that control the skeletal muscles are part of the motor division of the peripheral nervous system (PNS). The other part of the PNS is the sensory division, containing neurons that convey sensory information to the brain and spinal cord. In addition to motor and sensory neurons, the CNS consists of interneurons that connect sensory neurons to motor neurons and are interconnected by a large number of synapses. As for muscle fibers, neurons can be stimulated to convey an action potential that travels along the cell membrane. When a neural signal is conveyed from one neuron to another, the action potential is triggered by the migration of signal substances, neurotransmitters, in the synapses between the neurons. However, neurons can act either to excite or inhibit the generation of action potentials in their connection to other neurons; the combined excitatory and inhibitory stimuli determine whether an action potential is generated and whether the neural signal is passed through. This process in the interneurons of the CNS is responsible for conscious voluntary actions in humans, as well as automated responses such as postural motor control.

In motor neurons, the action potentials are generated in the CNS and conveyed to the muscles, which initiates muscle contractions. For sensory neurons, the signal starts at a sensory receptor. Of particular importance for motor control are the proprioceptors which provide information about the position of the limbs. Examples of proprioceptors are muscle spindles which react to muscle length change and Golgi tendon organs sensitive to tendon stretch. For the maintenance of posture, the vestibular organs of the ear are important as they monitor the spatial orientation of the head, to which visual input also contributes. In general, in healthy humans all three sensory systems, proprioceptive, vestibular, and visual, are complimentary, and therefore loss of some functionality can be compensated by increased reliance on other systems (Winter 1995).

The conduction speed of an action potential in an axon depends on the size of the axon and whether the axon has a myelin sheath that increases the conduction speed. For neurons involved in motor control tasks, conduction speeds of over 100 m/s can be found (Marieb and Hoehn 2010). However, as the axonal parts of the neurons in the PNS can be up to a meter in length, the transmission of a neural signal still takes a finite amount of time. In addition, the chemical synapse that connects two neurons can require 0.3–5 ms to transfer a neural signal (Marieb and Hoehn 2010). Therefore, a neural delay is associated with the transfer of a neural signal; it increases for distal muscles and sensory organs.

### 2.3 Motor Control

Human motor acts can be divided into two categories, which in general are combined in the performance of actual movements (Massion 1992). The first type is the maintenance of a reference position, also called postural control. Here the CNS applies stabilizing muscle activations, often without conscious awareness such as during quiet standing. The other type of motor act is the goal directed movement, in which a limb is moved along a trajectory toward a pre-determined goal.

In postural control tasks the musculoskeletal system and CNS act in a closed-loop, in which information about the current state of the system, *e.g.* center of mass of the trunk relative to the feet (Winter 1995), is used to generate stabilizing muscle activations. A simplified representation of a closed-loop system for postural control is shown in Figure 4. A desired reference position,  $r(t)$ , which is usually constant in time for postural control tasks, is compared with the present state of the body,  $y(t)$ . The state of the body is provided by the sensory part of the PNS; if the body is perturbed from the desired position, the CNS generates compensating motor commands proportional to the deviation.

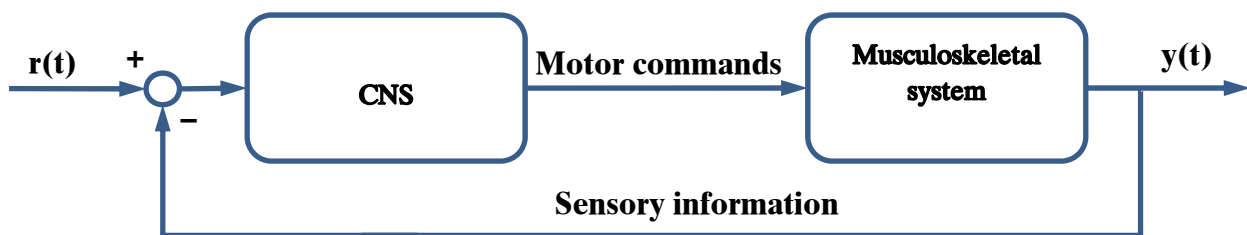


**Figure 4. Simplified representation of the closed-loop postural control system.**

Sensory information that is used for postural control comes from the muscle spindles or Golgi tendon organs for example (de Vlugt *et al.* 2006). In many muscles, muscle spindle sensory neurons are connected to the motor neurons in the spinal cord; with short latencies they can induce a contraction in the muscle when it is lengthened. This stretch reflex can be observed for the quadriceps muscles of the thigh, which automatically contract by a direct reflex arc between the muscle spindles and the motor neurons when lengthened. The patellar stretch reflex of the quadriceps help humans maintain an upright posture without conscious efforts as the knee is prevented from folding under the body weight (Marieb and Hoehn 2010). Muscle spindle reflexes may not only induce contraction of muscles, they may also lead to inhibitory stimuli of antagonistic muscles.

However, postural control does not depend only on low level reflexes. The sensory information gathered from the proprioceptors is relayed to higher levels in the CNS, where it is integrated and provides proprioception, *i.e.* it enables humans to know where a limb is positioned without seeing it. The integrated proprioceptive

information, together with visual and vestibular information, is used for whole body postural control. In this thesis work, joint angle sensors are used to generate posture maintaining muscle activations. No such sensors exist in the human body, but the integrated proprioceptive information provides the CNS with this information (Winter 1995). The exception is the head, for which the vestibular organs act precisely to provide spatial orientation.

Closed-loop control is an energy efficient way for the human body to achieve postural control, as muscles only are activated when required to counteract a disturbance (de Vlugt 2004). However, reflexive feedback is not the only control strategy present in human postural control. Muscle co-contraction plays an important role, because when antagonistic muscles are activated around a joint, although no net-moment is generated, the intrinsic stiffness and damping of the joint increases significantly due to the force-velocity and force-length relation of muscles described in Section 2.1. Muscle co-contraction of the trunk flexors and extensors has been shown to increase the stability of the lumbar spine (Hodges 1999), and to be present in postural control of the upper extremities (de Vlugt *et al.* 2002; de Vlugt *et al.* 2006). In impact biomechanics research it has been shown that, although reflex muscle activation is too slow to affect the outcome in 2–6.5 g volunteer impact tests, lower extremity muscle co-contraction prior to the impact significantly changed the restraint interaction forces (Begeman *et al.* 1980).

Closed-loop feedback control and co-contraction play important roles in posture maintenance tasks, but for goal directed movements, feedback control has been shown to be insufficient to explain observed human performance in rapid movements (Gerdes and Happee 1994). A reason for this is the neural delay associated with the transfer of sensory information and motor commands to and from the CNS, as delays reduce the stability of closed-loop systems. Goal directed movements are instead based largely on previous experience and expectations of the task; based on this the CNS generates a muscle activation scheme which is more of an open-loop type. Inverse internal models and ideal forward control have been proposed to explain how the CNS determines the muscle activation schemes. These models are supported by experiments in which arm motions are performed in an altered force field; after a few trials the test subjects are able to perform the motion as intended, but when the force field is restored again the test subjects have to re-learn the motion to perform it correctly (Kawato 1999). However, for most motor acts it is likely that a combination of open and closed-loop motor control is employed (Massion 1992), in such a way that the open-loop muscle activations are adjusted by closed-loop feedback if the goal directed movement deviates from the intended path.

Anticipatory postural responses are also associated with voluntary movements (Berg and Strang 2012). It has been found that in preparation to perform a task, such as lifting the arm or the leg rapidly, postural control muscles of the trunk, such as the transversus abdominis (Hodges 1999) and trunk flexors and extensors (Benvenuti *et al.*

1997), are activated first. The suggested effect of this is to stabilize the upright body to accommodate reaction forces associated with an arm or a leg movement (Massion 1992). It usually occurs 150–50 ms before activation of the muscles that initiate the movement of the limb (de Wolf *et al.* 1998).

Finally, the motor control of the human CNS is highly adaptive; in rear-end impacts volunteer test subject's muscular responses are attenuated and adapted rapidly with repeated trials (Blouin *et al.* 2003; Siegmund *et al.* 2003b). For the upper extremities in position control tasks, both length and velocity feedback gains have been found to change within seconds after a perturbation (de Vlugt *et al.* 2002). The adaptability of the CNS makes the investigation of human postural responses more challenging. In volunteer testing, habituation between repeated tests must be taken into account. For modeling purposes, it is possible that multiple model settings need to be validated under different conditions.



### 3 Review of Active Muscle Control in HBMs

The first implementations of muscle properties in HBMs were for cervical spine models (Deng and Goldsmith 1987; de Jager 1996; Wittek 2000). In some models, one dimensional or solid elements that represent only the passive elastic and damping response of the neck musculature was included (Jost and Nurick 2000; Robin 2001; Ejima *et al.* 2005; Toyota 2008). However, the active force generated by muscles is in a different order of magnitude than the passive stiffness and damping at physiological muscle lengths. Hence, models of active musculature have been included in numerous HBMs, summarized in Table 1.

The common method to implement active muscle properties is to utilize Hill-type line muscle elements, which are super-positioned in some models with a passive bulk material to provide 3D muscles (Behr *et al.* 2006; Hedenstierna *et al.* 2008; Iwamoto *et al.* 2009; 2011; 2012). The super-position method is used to generate 3D muscle geometry with existing material models in the FE solvers; it is possible to implement the Hill-model with local fiber directions in a continuum FE material model (Khodaei *et al.* 2013).

Two methods to find the activation level for the muscle material model have been used: Open-loop control, in which the muscle activation functions are defined prior to the simulation, or closed-loop feedback control in which the muscle activations are proportional to a variable in the model, *e.g.* the position of a limb.

**Table 1. Summary of HBM studies that have included active musculature.**

<b>Model Type / Solver</b>	<b>Reference</b>	<b>Body part</b>	<b>Actuators<sup>1</sup></b>	<b>Control</b>	<b>Activation scheme</b>	<b>Application</b>
<i>Active THUMS</i>	Sugiyama <i>et al.</i> 2007	Lower extremity	1D muscles	Open-loop	Inverse dynamics model	Brake pedal impacts
FE / LS-DYNA	Iwamoto <i>et al.</i> 2009	Upper extremity	3D muscles	Open-loop	Engineering judgment	Lateral impact to elbow
	Iwamoto <i>et al.</i> 2011	Whole body	3D muscles	Open-loop	Normalized EMG	Frontal impact
	Iwamoto <i>et al.</i> 2012	Whole body	3D muscles	Open-loop	Reinforcement learning model	Frontal and rear-end impacts
<i>TNO Active Human Model</i>	Cappon <i>et al.</i> 2007	Spine	Torque actuators	Closed-loop	PID controllers	Reversible belt pre-tension, roll-over
	Budziszewski <i>et al.</i> 2008	Upper extremity	1D muscles	Closed-loop	PID controllers	Elbow flexion
MB / MADYMO	Meijer <i>et al.</i> 2008	Spine, left arm and legs	Torque actuators, 1D muscles	Open and closed-loop	PID controllers, Engineering judgment	Far-side impact
	Fraga <i>et al.</i> 2009	Cervical spine	1D muscles	Closed-loop	PID controllers	Motorcycle braking and cornering
	Nemirovsky <i>et al.</i> 2010	Cervical spine	1D muscles	Closed-loop	PID controllers	Rear-end impacts
	van Rooij 2011	Spine	Torque actuators, 1D muscles	Closed-loop	PID controllers	Autonomous braking
	Meijer <i>et al.</i> 2012	Whole body	1D muscles, torque actuators	Closed- and open-loop co-contraction	PID controllers, variable co-contraction	Autonomous braking, frontal, lateral, and rear-end impact
	Meijer <i>et al.</i> 2013b	Whole body, hip and elbow added	1D muscles, torque actuators	Closed- and open-loop (co-contraction)	PID controllers, variable co-contraction and reaction time	Pendulum impacts, car braking, sled impacts
	Meijer <i>et al.</i> 2013a	Whole body, new neck and elbow	1D muscles, torque actuators	Closed- and open-loop (co-contraction)	PID controllers, varied levels of co-contraction	Anterior-posterior T1 perturbations, elbow flexion impulses, and autonomous braking.

**Table 1 continued.**

<b>Model Type / Solver</b>	<b>Reference</b>	<b>Body part</b>	<b>Actuators<sup>1</sup></b>	<b>Control</b>	<b>Activation scheme</b>	<b>Application</b>
MB /MADYMO	Bose and Crandall 2008 Bose <i>et al.</i> 2010	Lower extremities, elbow, and neck	1D muscles, static joint torques for the neck	Open-loop (co-contraction only)	Optimization	Frontal impact whole body injury assessment
FE / PAM-CRASH	Choi <i>et al.</i> 2005	Upper and lower extremities	1D muscles	Open-loop	Normalized EMG	Occupant bracing in frontal impacts
FE / Radioss	Behr <i>et al.</i> 2006	Lower extremity	3D muscles	Open-loop	Normalized EMG	Emergency braking, frontal impact
MB / MADYMO	de Jager 1996, van der Horst 2002	Cervical Spine	1D muscles	Open-loop	Reflex activation	Frontal, lateral, and rear-end impacts
FE /PAM-CRASH	Wittek 2000	Cervical spine	1D muscles	Open-loop	Reflex activation	Rear-end impacts
FE / LS-DYNA	Brolin <i>et al.</i> 2005; 2008	Cervical spine	1D muscles	Open-loop	Reflex activation, Optimization	Frontal and lateral impact, helicopter crash
FE / LS-DYNA	Hedenstierna 2008	Cervical spine	3D muscles	Open-loop	Reflex activation, Optimization	Frontal, lateral and rear-end impacts
MB / LS-DYNA	Chancey <i>et al.</i> 2003, Dibb <i>et al.</i> 2013	Cervical spine	1D muscles	Open-loop	Optimization	Tensile neck loading, frontal impact, Child HBM

<sup>1</sup> In all HBMs which used muscle elements as actuators, the active behavior was modeled with a Hill-type material model. All the models with 3D muscles employ the super-position of a passive continuum bulk material and Hill-type line muscle elements (Hedenstierna *et al.* 2008).

### **3.1 Open-loop Muscle Activation**

Open-loop control means that the control signal is not continuously updated based on measured information about the state of the process being controlled, but rather on a known state and a model for the response of the system. In the context of previously developed HBMs this means that the muscle activations as a function of time are defined prior to the simulation. The outcome is observed afterwards, and the activation function may be adjusted to achieve a better model response in upcoming simulations.

#### **3.1.1 Reflex Activation**

Several cervical spine models (de Jager 1996; Wittek 2000; van der Horst 2002; Brodin *et al.* 2005) have accounted for the influence of active behavior by the application of a maximum activation starting at a specified time in the simulation. This models a reflexive startle response that is determined by the choice of time constants in the activation dynamics model or by the shape of the pre-defined activation level curve. With this approach in an MB neck model, de Jager (1996) showed the importance of active muscles to capture the human head-neck response in frontal and lateral impacts; the same model was later refined and employed in rear-end impacts, and the importance of active muscles was yet again shown by van der Horst (2002). Wittek (2000) and Brodin *et al.* (2005) used this approach combined with Hill-type line muscle elements in an FE neck model; they studied the protective effect of the neck muscles on cervical facet joint injuries in rear-end impacts and on soft tissue injuries in frontal and side impacts, respectively.

#### **3.1.2 Optimization of Static Posture-Maintaining Activations**

Chancey *et al.* (2003) developed an MB neck model with detailed muscles and studied the effect of muscle activation on tensile loading of the neck for two sets of muscle activations. The muscle activations evaluated were determined with an optimization scheme that gave an initial stable posture for relaxed and maximal muscle tension. More recently the same method was applied to find posture maintaining muscle activation schemes for six and ten-year-old pediatric cervical spine models (Dibb *et al.* 2013). The neck stabilizing muscle activation levels reported by Chancey *et al.* (2003) were used as a starting point to find load case specific stabilizing activations in a study with an FE neck model conducted by Brodin *et al.* (2008). The model was then applied to evaluate the influence of muscle tension on spine injuries in helicopter accident scenarios. Bose and Crandall (2008) and Bose *et al.* (2010) used an MB HBM which was varied in size from the approximate 20<sup>th</sup> to 80<sup>th</sup> percentile male anthropometry, nine different initial postures, and 0–100% muscle co-contraction in Hill-type line elements. They performed optimizations to generate static stabilizing co-contraction activation levels and evaluated the influence of initial muscle co-contraction on a whole body injury metric in a simulated 57 km/h impact. They found that the initial posture was the most significant factor in determining the injury outcome, but that

initial muscle co-contraction also had some influence. In particular, an increased risk for injury in the lower extremities with increasing muscle co-contraction was reported.

### 3.1.3 Optimization of Dynamic Activations

Iwamoto *et al.* (2012) presented a version of the THUMS HBM with a detailed 3D representation of muscles for all body parts. For the head and neck, a simplified model using only 1D Hill-type elements was also developed. Using the simplified neck model and an optimization process called reinforcement learning, tabulated muscle control functions that account for both joint angles and velocities were derived. The optimization provided individual muscle activation functions that were applied in the detailed model in a rear-end impact test case. With the reinforcement learning activations the model appeared to be better than the passive model in the initial phase of the impacts, but then it overestimated the effect of muscles on the kinematics.

### 3.1.4 Estimation based on Experimental Data

Behr *et al.* (2006), Sugiyama *et al.* (2007), and Chang *et al.* (2008) all modeled emergency braking with active muscles in the lower extremities. The muscle activation levels were taken from normalized EMG measurements in emergency braking experiments. They studied the injury risk in frontal impacts (Behr *et al.* 2006), brake pedal impacts (Sugiyama *et al.* 2007) and knee impacts (Chang *et al.* 2008), and concluded that the inclusion of active musculature changes the injury risk in these situations. Chang *et al.* (2008) predicted that the external force causing a fracture to the knee-thigh-hip area decreases when muscle tension is taken into account, but that a limitation of the study was the lack of detailed muscle activation data for the lower extremities. Therefore, a second study was made (Chang *et al.* 2009), in which a detailed inverse dynamics musculoskeletal model was used to derive detailed individual muscle activations from experimental data. The same approach with inverse optimization was used by Choi *et al.* (2005), *i.e.* an optimization in which muscle activations are derived using a musculoskeletal model, measured forces, and limb positions, together with hypothesized optimization constraints. They simulated occupant bracing in sled impacts with active muscles in the upper and lower extremities.

## 3.2 Closed-loop Muscle Activation

In closed-loop applications the response of the controlled systems is continuously monitored and the control signal is adjusted in accordance with the actual model response. In the human body the reflex arc, described in Section 2.3, is the simplest closed-loop structure. In engineering science, closed-loop control is often achieved by a proportional, integral, and derivative (PID) controller defined as:

$$e(t) = r(t) - y(t) \quad (1)$$

$$u(t) = k_p \cdot e(t) + k_i \cdot \int_0^t e(\tau) d\tau + k_d \cdot \frac{de(t)}{dt}. \quad (2)$$

The current state of the system,  $y(t)$ , is compared with the reference,  $r(t)$ , and the control signal,  $u(t)$ , is proportional to the difference between the two according to Equation (2). The characteristics of the PID controller are determined by the proportional gain,  $k_p$ , integral gain,  $k_i$ , and derivative gain,  $k_d$ . The PID feedback control can be applied to model human postural responses; it is then hypothesized that proportional and derivative feedback represent muscle spindle and vestibular reflexive stabilization, while the integrative controller counteracts gravity. In the AHBM developed in this thesis, PID feedback control to model postural responses is utilized in Papers I–II and V–VI.

### 3.2.1 Torque Actuators

One of the first implementations of closed-loop feedback to model occupant responses was done by Cappon *et al.* (2007) who utilized PID controllers to control the moment applied for each individual vertebral joint in an MB HBM. First, a simulation in which the vertebral joints were locked to each other was made. The static moments generated in each joint were extracted and used as initial moments for tuning simulations. Next, PID controller gains were chosen by optimization so that the difference between model responses and those of volunteers impacted by a pendulum was minimized. The model was then applied to simulate the phase preceding a roll-over accident and a static application of a reversible pre-tensioned restraint. The addition of the active spine improved the model kinematics in the roll-over scenario but was less successful in capturing the volunteer response to the reversible pre-tensioned restraint. The spine with active torque actuators was later utilized in several publications on the *TNO Active Human Model* (Meijer *et al.* 2008; van Rooij 2011; Meijer *et al.* 2012; Meijer *et al.* 2013a; 2013b) developed by the Netherlands Organization for Applied Scientific Research with the official acronym TNO. A similar approach was also used by Almeida *et al.* (2009), who implemented PID feedback controlled torque actuators in a numerical model of the frontal-impact ATD THOR. They concluded that the model with a feedback controlled head and neck complex was better than its passive counterpart in capturing occupant kinematics in both lateral and longitudinal acceleration driving scenarios.

### 3.2.2 Line Muscle Elements

Budziszewski *et al.* (2008) implemented closed-loop control of 1D Hill-type elbow flexor and extensor muscles in a MB arm model. A PID controller was implemented for the elbow joint for which the muscles were divided in flexors and extensors and assigned equally large activations from the controller. The model was tested and compared with experimental data of voluntary elbow flexion and extension; it was concluded that the kinematic performance of the model matched that of the volunteers but that predicted muscle activation levels were over-estimated. Fraga *et al.* (2009) used feedback PID control of line muscle elements to stabilize the head of a motorcycle rider in lateral and longitudinal maneuvers for MB simulations. They concluded that their model appeared to capture the resulting head kinematics of a volunteer of average awareness when braking a motorcycle. Furthermore, they stated

that the model is promising for the development of advanced restraint systems for motorcycle riders, and that it is a step towards fully active HBMs.

The head-neck model used by Fraga *et al.* (2009) was further developed by Nemirovsky and van Rooij (2010) by the implementation of a postural controller for the head-neck complex, with the aim of regulating flexion-extension, lateral flexion, and rotation of the head. The motions were decoupled by a muscle recruitment strategy, which would ensure that only one degree of freedom was influenced by each controller; however, only the model response in flexion-extension was evaluated. Along with three PID controllers for the three head rotation degrees of freedom, a variable co-contraction ratio controller was implemented. The co-contraction ratio was important for the resulting closed-loop response, as muscular co-contraction makes a large contribution to the damping of the closed-loop system. The model was later used by van Rooij (2011), who hypothesized that the attentiveness of drivers is reflected by the gains used in the control model. He simulated the influence of different levels of awareness on driver kinematics in autonomous braking interventions.

Meijer *et al.* (2012) integrated and extended the work presented in the previous publications on the *TNO Active Human Model* (Cappon *et al.* 2007; Meijer *et al.* 2008; Fraga *et al.* 2009; Nemirovsky and van Rooij 2010; van Rooij 2011) to form a complete model. The feedback loop was complemented with a reaction time for events that cause a larger controller error than the preceding ones in the simulation. A low-pass filter function representing the neural transmission time from the CNS to the distal muscles was also added. The signal from each controller is converted to the muscles or torque actuators by multiplication with a constant defined in a recruitment table, to ensure that only the degree of freedom being regulated is affected (Nemirovsky and van Rooij 2010). Furthermore, muscle co-contraction can be defined prior to the simulation, *i.e.* open-loop, generating muscle tension without any net moment around the joints, contributing to the intrinsic stiffness. The kinematic responses of the model were evaluated for autonomous braking, frontal, lateral, and rear-end impacts. It was concluded that both feedback control and muscle co-contraction is needed to predict volunteer responses in these types of events.

In Meijer *et al.* (2013b), feedback controlled elbow and hip muscles were introduced; it was stated that a muscle recruitment approach similar to that described by Nemirovsky and van Rooij (2010) was used to decouple hip flexion-extension, medial-lateral rotation and abduction-adduction. Utilizing 50% co-contraction of the muscle actuators, the model was reasonably well able to capture forward displacements of the chest and neck in 1 g driver braking events, and in 3.8 g, and 15 g volunteer impact tests. Meijer *et al.* (2013a) introduced new neck muscle geometry in the *TNO Active Human Model*, and evaluated the response of the head-neck complex to low level random perturbations of the T1 vertebrae. Furthermore, force pulse perturbations were applied to the hand, inducing flexion and extension of the elbow and the model response was compared with that of one volunteer. Finally, the difference between a

braced state and a relaxed state for the model was evaluated by the simulation of a braking event. It was concluded that the model response for the relaxed condition is different from the braced condition.

## 4 Review of Volunteer Tests of Muscle Responses

A brief review of studies to investigate the influence of muscle activation on volunteer kinematics is given here. The emphasis is on pre-crash loads, typically below 1.5 g and with durations of at least 0.2 s. Some volunteer tests to study the human response to low impact loads are also included.

### 4.1 Frontal Impacts and Braking Scenarios

Volunteer responses to frontal impact pulses and braking decelerations have been studied using sled and linear sled setups for accelerations ranging from 0.2–5 g for 0.2–0.6 s (Ejima *et al.* 2007; 2008; 2009; Arbogast *et al.* 2009; Bae *et al.* 2010; Beeman *et al.* 2011). Typically two types of instructions are given to the volunteers: Either to be initially relaxed or to be maximally tensed to brace for the upcoming acceleration pulse. The general result of these studies is that the presence of muscular contraction influences the kinematics of a volunteer significantly. For instance, bracing by co-contraction before impact reduces forward displacements 36–69% for different body parts; for the head in particular forward displacement is reduced from 169 mm to 107 mm in a 5 g impact (Beeman *et al.* 2011). In addition, Ejima *et al.* (2007; 2008; 2009) found muscle reflex activities 100–130 ms after acceleration onset; for testing with loads of 0.8 g over 0.6 s, the reflexive response was concluded to be fast and large enough to affect the volunteer's kinematics in the test (Ejima *et al.* 2009).

Occupant kinematic responses to braking deceleration loads have also been investigated in a test vehicle setting. For instance, Carlsson and Davidsson (2011) used planar film analysis to quantify forward displacements of drivers and passengers due to autonomous brake interventions of 0.3 g, 0.4 g, and 0.5 g over 1.5 s while driving on ordinary roads. They found a mean forward head displacement of 96 mm, with a standard deviation of 47 mm for all conditions; taller volunteers had larger forward head displacement and females who were of approximate 50<sup>th</sup> percentile male stature showed larger forward displacement than their male counterparts. Van Rooij *et al.* (2013) conducted experiments with a professional driver on a test track. They evaluated the differences in forward head displacements for driver voluntary braking, autonomous braking, and autonomous braking with a distraction, in the form of sending a text message from a cell phone. A significant difference in the driver's forward head displacements was found for the driver braking and the autonomous braking scenarios. This was hypothesized to be caused by the driver's anticipation in the voluntary braking case.

Morris and Cross (2005) made a qualitative study in which occupant responses to pre-crash braking were classified based on recordings from five cameras monitoring the passenger seat of a car driving on a test track. They found that bracing behavior, defined as holding on to a part of the vehicle structure firmly with the hand or with part of the arm, occurred only in a minority of events with belted passengers. It was more predominant the longer the duration of the pre-impact event and when the volunteer was already holding on to the structure prior to the event. Behr *et al.* (2010)

combined joint angle measurements during driver maximum braking, in a driving simulator with lower extremity EMG data recorded in emergency braking tests performed in a test vehicle. Emergency braking was tested by throwing a ball in front of the vehicle without prior notification to the volunteer drivers. Muscle activation levels for the lower extremity muscles, joint angles, and brake pedal forces were reported and suggested to be a standard initial condition for frontal impacts preceded by driver emergency braking.

## **4.2 Lateral Impacts and Vehicle Maneuvers**

Ejima *et al.* (2012) conducted volunteer sled tests with 0.4 g and 0.6 g lateral accelerations over 0.6 s. They found that, just as in frontal impact and braking scenarios, muscle tension prior to the event affected the occupant kinematics. The angle change of the torso relative to the seat was reduced by 5° for the lower acceleration level and by 10° for the higher level, for a tensed initial condition compared with a relaxed. In this lateral acceleration study, only a lap belt was utilized to secure the occupant to the test seat. Lower extremity muscle activations and foot rest forces were found, indicating that the lower extremities play a role in the seated occupant postural response to lateral accelerations.

In lateral vehicle maneuvers, such as avoidance steering maneuvers, the occupant loading will have multiple components: a lateral acceleration component, one due to the yaw rate of the vehicle, and possibly also one due to roll of the vehicle body. This is captured when testing is conducted in a test vehicle (Muggenthaler *et al.* 2005; Huber *et al.* 2013). Muggenthaler *et al.* (2005) performed sinusoidal steering tests with first a human volunteer and then a Hybrid III ATD in the passenger seat, with a lateral acceleration amplitude of 0.5 g. In addition, 0.6 g lane change maneuvers with human volunteers as passengers and drivers were carried out. They concluded that the volunteers displayed both voluntary and reflex muscle activation; their responses were much more flexible than those of the ATD. Huber *et al.* (2013) conducted lane change maneuvers with a lateral acceleration of 1 g. They identified muscle onset, 0.11–0.17 s after initiation of the steering maneuver, by using surface EMG electrodes on their volunteers, who were riding in the passenger seat of the test vehicle.

## **4.3 Rear-End Impacts**

The most thorough investigations of the effects of muscular contraction on occupant kinematics have probably been made for rear-end impacts (Szabo and Welcher 1996; Ono *et al.* 1997; Magnusson *et al.* 1999; Brault *et al.* 2000; Hell *et al.* 2002; Blouin *et al.* 2003; Siegmund *et al.* 2003a; Siegmund *et al.* 2003b; Siegmund *et al.* 2004). All of these studies focus on whiplash injuries, *i.e.* neck injuries with low initial severity level but with high risk of long term impairment. Epidemiological studies show that whiplash injury occurs in relatively mild rear-end impacts; for example, Kullgren *et al.* (2003) found that for 7 g rear-end impacts in real accidents the whiplash injury risk was approaching 100%. Impact pulses of 0.4–6.3 g with durations of 0.06 to 0.15 s have been applied in the volunteer tests mentioned above. Even though the duration in

these rear-end impact studies is quite short, they show that muscle contraction plays a role in rear-end impacts: that there is somato-sensory triggering of the neck muscles due to lumbar spine acceleration (Szabo and Welcher 1996; Magnusson *et al.* 1999); that volunteers subjected to multiple test pulses habituate (Blouin *et al.* 2003; Siegmund *et al.* 2003b); that muscle injury is possible due to eccentric contraction (Brault *et al.* 2000).

#### **4.4 Driving Simulators**

Driving simulators provide an opportunity to generate a pre-crash situation that includes an actual collision threat. Hetier *et al.* (2005) simulated an accident caused by a truck overtaking a tractor on a two lane road and evaluated occupant postures at the time of impact. They found that in general their volunteers were out of position relative to standardized crash test positions. For instance, 67% had moved backwards in anticipation of the crash and 30% had their left arm in front of the air bag. A similar study was published by Hault-Dubrulle *et al.* (2011), who found a bracing response, in combination with emergency braking, characterized by the volunteers extending their elbow and knee joints, pushing themselves backward into the seat. However, in both of these studies, a fixed platform simulator was used. Hence, the volunteer kinematic responses found were not affected by the acceleration load that would be present during actual emergency maneuvers.



## 5 Summaries of Appended Papers

Brief summaries of the publications appended to this thesis are given here. The full papers are appended at the end of the thesis.

### 5.1 Paper I

The aim of Paper I is to address the challenges of implementing postural feedback control with a muscle material model in an FE HBM. A musculoskeletal model was developed, using the right upper extremity of the FE HBM THUMS v3.0 (Toyota 2008), however, the original contact-based elbow joint of the HBM was replaced with a kinematical revolute joint. Postural feedback control was achieved by the implementation of a PID controller and a muscle activation dynamics model, see Figure 5. Furthermore, simulations of volunteer tests with low impact loads, resulting in elbow flexion motions, were conducted.

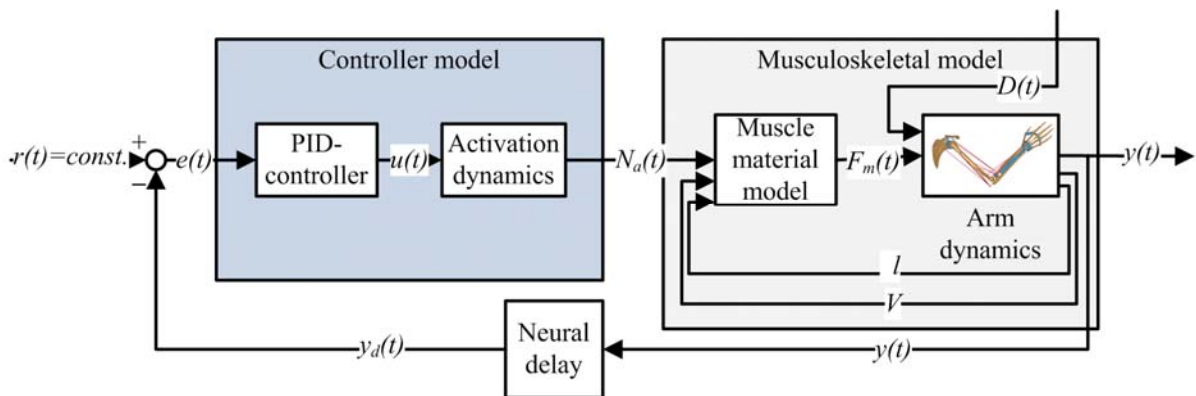


**Figure 5. Illustration of the neuromuscular feedback control loop implemented in Paper I.**

The results showed that the musculoskeletal model strength and passive stiffness characteristics were comparable to experimental data in the literature. The feedback control loop implemented was able to stabilize the model in simulations with gravity, thus the model could maintain posture. Simulation of volunteer experiments showed that, by a variation of controller gains, different kinds of instructions to the volunteer could be captured by the model. Simulations with the original contact-based joint showed that lower controller gains were necessary, due to an increase in phase lag, and that 3D joint motions had to be controlled with a 1D reference signal.

The result from simulations of volunteer responses indicated that, by variation of the controller gains, it is possible to simulate, with an FE HBM, the various active muscle responses that can be expected in the pre-crash phase. Comparison of simulations with the two joints in the model showed that feedback control can be used in an FE HBM, but that joint definitions should be modeled in more detail to capture human-like passive joint properties. In conclusion, the study in Paper I showed that it is possible to use feedback control of a non-linear musculoskeletal model in an FE environment to obtain a posture maintaining HBM and to simulate reflexive muscle responses.

## 5.2 Paper II

The aim of Paper II is to model passenger kinematics in an autonomous braking event by using an FE HBM with active muscles. Paravertebral muscles of the lumbar and cervical spine, superficial muscles of the neck, and the abdominal muscles were added to the FE HBM THUMS v3.0 (Toyota 2008), see Figure 6. Active control was implemented using three PID controllers, for the head, the neck, and the lumbar segment angles, see Figure 6. Volunteer kinematic data from sled tests (Ejima *et al.* 2007) and from occupants in the front passenger seat during autonomous braking interventions (Carlsson and Davidsson 2011) was sampled for comparison with HBM simulation results.

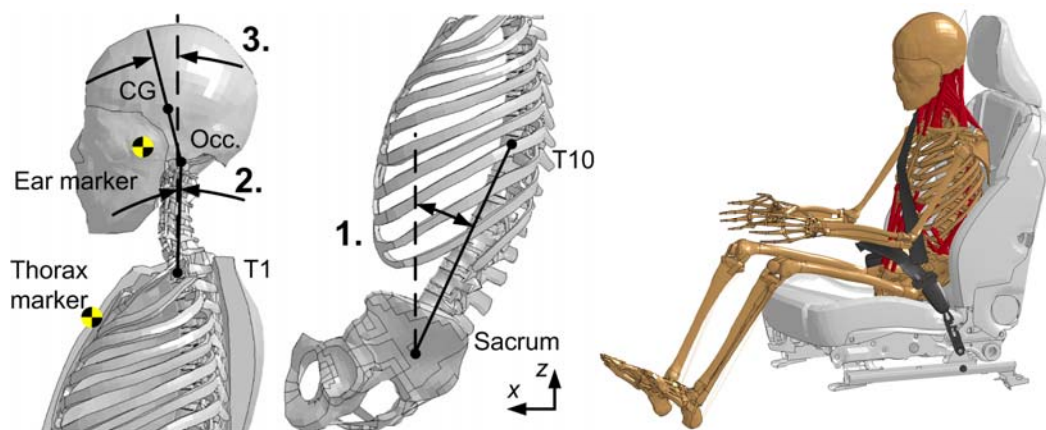


**Figure 6. The angles utilized for the feedback control of the (1) trunk, (2) neck, and (3) head muscles (left). The THUMS HBM with trunk and neck musculature added (right).**

The results showed that the HBM captured the characteristics of the kinematics of volunteers in sled tests. Peak forward displacements have the same timing as for the volunteers, and lumbar muscle activation timing matches data from one of the volunteers. The responses of volunteers in autonomous braking interventions are mainly small head rotations and translational motions. This is captured by the HBM controller objective, which is to maintain the initial angular positions. The HBM response with active muscles is within one standard deviation of the average volunteer response with respect to head displacements and angular rotation.

It was concluded that, with the implementation of feedback control of active musculature in an FE HBM, it is possible to model the occupant response to autonomous braking interventions. The lumbar controller is important for the simulations of lap belt-restrained occupants; it is less important for the kinematics of occupants with a modern 3-point seat belt. Increasing head and neck controller gains provides a better correlation for head rotation, whereas it reduces the vertical head displacement and introduces oscillations.

### 5.3 Papers III and IV

The primary aim of Papers III and IV is to generate sets of validation data for HBMs that are intended for the simulation of occupant responses in braking events. Secondary aims are to evaluate the effect of reversible seat belt pre-tension on occupant kinematics and muscle responses, and to compare autonomous braking with voluntary driver braking.

Eleven male and nine female volunteers, driving a passenger car on ordinary roads, performed maximum voluntary braking; they were also subjected to autonomous braking events with both standard and reversible pre-tensioned restraints, both as drivers (Paper III) and passengers (Paper IV), see Figure 7. Kinematic data was acquired by film analysis, and surface EMG signals were recorded bilaterally for muscles in the neck, the upper extremities, and lumbar region. Maximum voluntary contractions (MVCs) were carried out in a driving posture for normalization of the EMG. Seat belt positions, interaction forces, and seat indentions were measured.

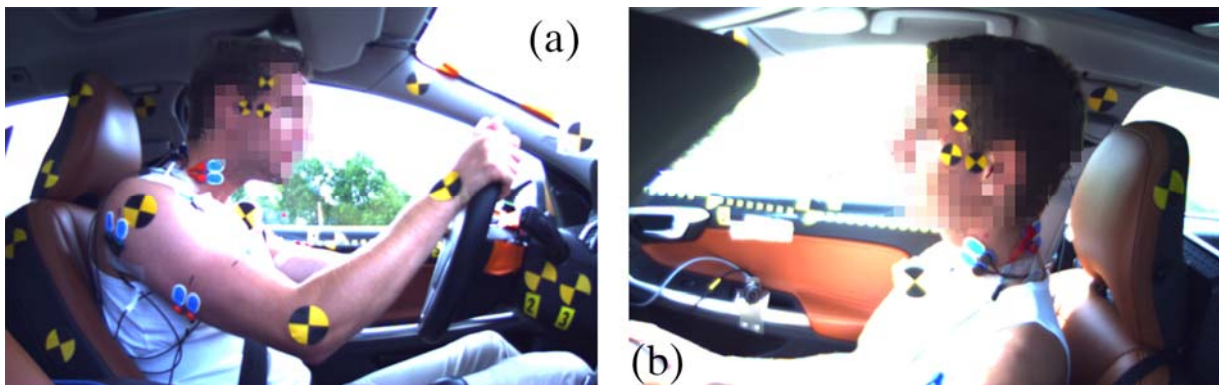


**Figure 7. Instrumented volunteer in (a) the driver seat (Paper III) and (b) the passenger seat (Paper IV).**

In total, five sets of validation data for human models intended to represent occupant pre-crash responses were obtained: for autonomous braking with pre-tensioned and standard restraints in both the driver and passenger positions, and for driver voluntary braking. It was found that seat belt pre-tension affects the kinematic and muscle responses of both drivers and passengers during autonomous braking. For passengers, a statistically significant reduction in head and torso forward displacement was found with a pre-tensioned belt in comparison with a standard belt, *e.g.* 118 mm compared with 194 mm for the head of male passengers. For drivers, the influence of the volunteer braking on his or her own was larger than the influence of belt pre-tension. There was a reduction in female head forward displacements from 116 mm, with a standard belt in autonomous braking, to 38 mm in driver braking. With the pre-tensioned seat belt, muscle activity was induced by the belt pre-tension rather than the acceleration onset, as for the standard belt in autonomous braking. The muscle and kinematic response invoked by the belt pre-tension had characteristics that could be due to a tactile startle reflex.

## 5.4 Paper V

The aim of Paper V is to study driver and passenger kinematics in autonomous braking scenarios with and without pre-tensioned seat belts, using a whole-body FE HBM with active muscles. In addition to the feedback controlled muscles for the trunk and neck (Paper II), feedback control and upper extremity musculature for the elbow and shoulder flexion-extension was added to the HBM, see Figure 8. Controller gains were found using a radial basis function meta-model sampled by 144 simulations of an 8 m/s<sup>2</sup> volunteer sled test. The HBM kinematics, interaction forces, and muscle activations were validated for the passenger and driver positions, with and without 170 N seat belt pre-tension, in combination with 11 m/s<sup>2</sup> autonomous braking deceleration (Papers III and IV). Then, the HBM was used for a parameter study in which seat belt pre-tension force and timing were varied from 170 N to 570 N and from 0.25 s before to 0.15 s after deceleration onset in an 11 m/s<sup>2</sup> autonomous braking scenario.

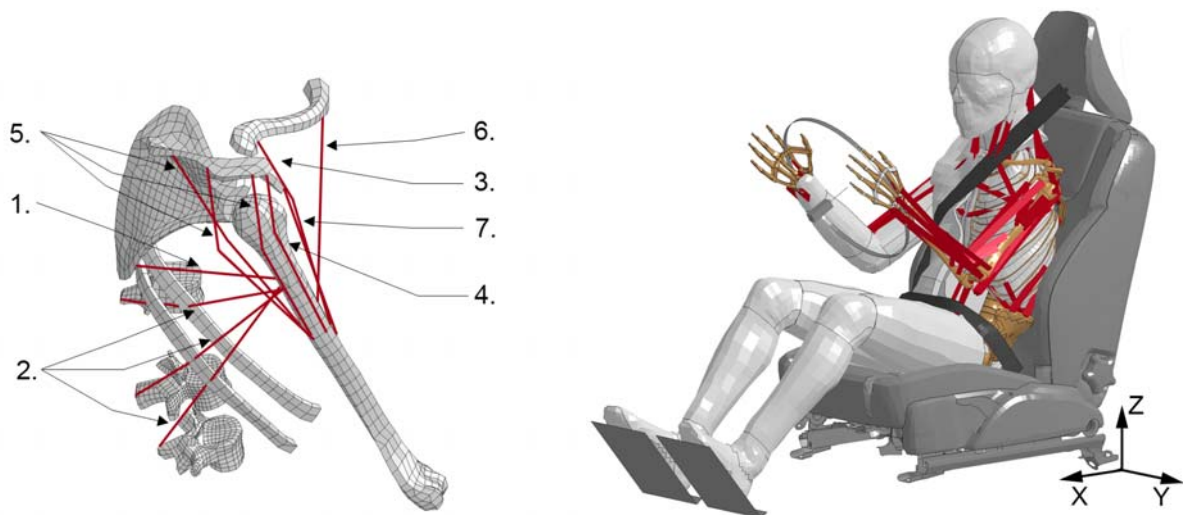


**Figure 8. Shoulder muscles implemented to model driver interaction with the steering wheel (Paper V) (left) and the HBM seated in the validation test setup (right). 1. Teres major; 2. Latissimus dorsi; 3. Anterior deltoid; 4. Middle deltoid; 5. Posterior deltoid; 6. Pectoralis major, clavicular head. 7. Coracobrachialis.**

The model validation showed that the forward displacements and interaction forces of the HBM correlated with those of corresponding volunteer tests. Muscle activations and head rotation angles were overestimated in the HBM in comparison with volunteer data. With a standard seat belt in 11 m/s<sup>2</sup> autonomous braking interventions, the HBM exhibited peak forward head displacements of 153 mm and 232 mm for the driver and passenger positions. When 570 N seat belt pre-tension was applied 0.15 s before deceleration onset, a reduction of peak head displacements to 60 mm and 75 mm was predicted. Driver and passenger responses to autonomous braking with standard and pre-tensioned restraints were successfully modeled with a whole-body FE HBM with feedback controlled active muscles. The displacement of the head relative to the trunk for the HBM is quite constant for all variations in timing and belt force. It is the reduced trunk displacements that lead to reduced forward head displacements.

## 5.5 Paper VI

The aim of Paper VI is to model the driver postural response in driver braking scenarios. In the analysis of the volunteer data (Paper III) it was noticed that the muscle and kinematic responses between the driver braking and autonomous braking test cases differ significantly. It was hypothesized that this difference is due to an anticipatory postural response during driver braking. This was modeled as a time dependent change in the reference value for the feedback controllers, which generates correcting moments to counteract the braking deceleration. In addition, lower extremity muscles were added to the whole-body FE HBM developed in Papers II and V, see Figure 9.

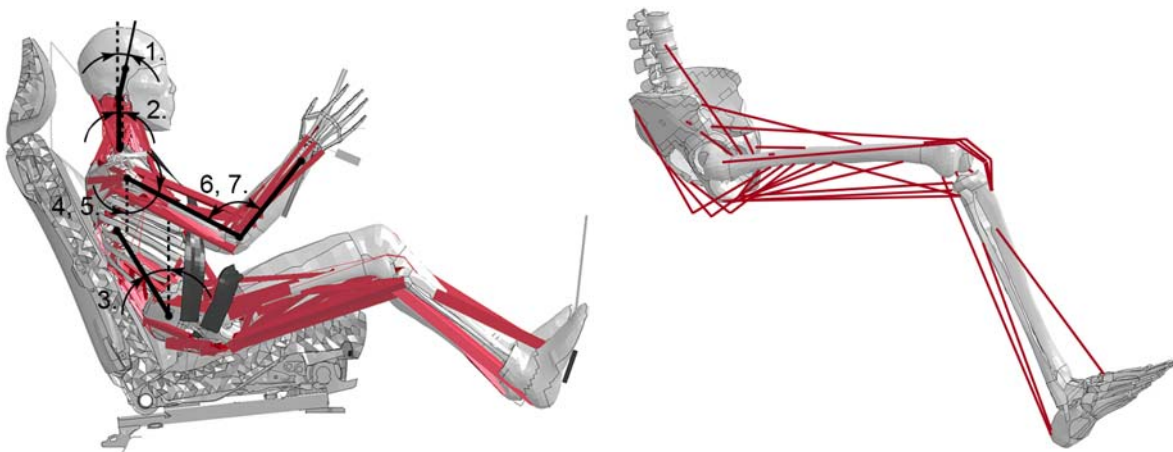


**Figure 9. Segment angles used for feedback control (Papers V and VI) (left); muscle implementation for the lower extremities (right). The (1) head, (2) cervical, (3) lumbar, and (4) and (5) shoulder angle controllers all use the angle of the body part with respect to the vertical axis, while the (6) and (7) elbow controllers utilize the relative angle between the humerus and ulna.**

The results showed that in  $11 \text{ m/s}^2$  driver braking simulations, the peak forward displacement of the head was decreased by 100 mm, of the shoulder by 30 mm, and head flexion rotation was decreased by  $16^\circ$ , compared with the HBM validated for modelling autonomous braking of the same magnitude. This means the HBM was within one standard deviation of corresponding test data from volunteers performing maximum braking. It was concluded that the hypothesized anticipatory responses can be modeled by changes of the reference positions of individual joint feedback controllers that regulate muscle activation levels. This method of modeling anticipatory postural reactions could have application for the simulation of other driver voluntary actions, such as emergency avoidance by steering.



## 6 Discussion

This thesis employs numerical modeling and volunteer testing to investigate car occupant muscle reactions and kinematics caused by pre-crash braking decelerations and belt pre-tension. A method for closed-loop feedback control to model occupant muscle responses in an FE AHBM was developed. Volunteer tests with occupants driving and riding in a car, subject to autonomous and driver braking interventions, were conducted. The volunteer tests not only provided validation data for the AHBM, but also indicated that driver postural responses are significantly different during voluntary and autonomous braking. The AHBM was employed to investigate this difference and it was found that a potential explanation is the presence of a hypothesized anticipatory postural response during driver voluntary braking. The combination of numerical modeling and volunteer testing in this thesis provides a better means for the understanding of car occupant muscle responses in pre-crash braking than either of the two approaches separately. The numerical modeling helps to define what parameters should be measured in volunteer tests, while the volunteer tests provide insight into actual car occupant muscle responses that can be implemented and evaluated in the HBM.

### 6.1 Model Development

The developed AHBM (Papers I–II and V–VI) is an FE model, based on the THUMS v3.0 (Toyota 2008). One dimensional Hill-type muscle elements were added to the model; for some of the shoulder and lower extremity muscles, the Hill-elements were coupled in series with seat belt elements to allow for a curved line of action. Muscle activation levels were controlled by PID feedback controllers that utilized joint angles to provide postural responses for the trunk, neck, head, and upper extremity muscles.

The strength of the FE method for impact biomechanics modeling of the human body lies in the capacity to predict injury at the tissue level, for instance to predict fractures (*e.g.* Chang *et al.* 2008; Chang *et al.* 2009). However, detailed FE models have high computational cost, which is why the MB HBM has an advantage when only the occupant kinematics is of interest. As summarized in Section 3.2, several studies have been published on the Active MB HBM utilizing feedback control to model pre-crash occupant responses. For future use of Active HBMs, it will be of interest to study events consisting of both the pre-crash phase and the crash phase, and to assess the risk of injury. With more powerful integrated systems, the risk of injuring vulnerable occupants, *e.g.* elderly people or children, will also have to be assessed in pre-crash simulations. Therefore, it will be important to be able to utilize FE HBMs in scenarios where muscle activation and postural responses have an influence on the occupant kinematics.

### 6.1.1 Postural Feedback Control in Finite Element HBMs

Human postural responses are governed to a large extent by feedback control, as described in Section 2.3. This has been utilized to model and explain human postural responses in many situations, from quiet standing (Barin 1989; Winter 1995) to random force perturbations to the upper extremities (de Vlugt *et al.* 2006). In this thesis work, it was demonstrated that postural feedback control can be used to model both car driver and passenger responses to autonomous braking interventions (Papers II and V) and elbow perturbations (Paper I).

The explicit FE software LS-DYNA (LSTC 2013) was utilized throughout this thesis. Explicit FE problems are characterized by short duration and non-linearly changing conditions, for example in the automotive industry for crash simulations in which structural parts engage and disengage in contacts. Feedback control utilizes information about the past state of the system to generate the control signals, which has been implemented only to a limited extent in LS-DYNA previously. Therefore, one of the aims of the work in Paper I was to evaluate the feasibility of feedback control in an FE HBM and in LS-DYNA. To achieve closed-loop PID control of the Hill-material model in LS-DYNA, the PID controller, neural delay, and activation dynamics functions (Paper I) were written in the programming language Fortran as part of the solution control subroutine (uctrl1) in a library of the LS-DYNA source-code (Erhart 2010). Since the FE HBM and the inclusion of muscle responses in HBMs are pointed out as important enablers in virtual testing of safety systems (IRCOBI 2006), the implementation of musculoskeletal feedback control in a solver utilized for FE HBMs is an important contribution of this thesis. There are also alternative approaches to implement feedback control in LS-DYNA, but they rely on coupling to other software such as Matlab/Simulink (The Mathworks Inc., Natick, MA, USA) or independently developed external programs (*e.g.* Prügler *et al.* 2011).

There are also some challenges related to the use of a Hill-muscle material in an FE model. An oscillatory behavior of the force of the Hill-elements was found (Paper I), similar to those reported in other HBMs (Wittek and Kajzer 1997; Hedenstierna *et al.* 2008). This is likely to be a problem related to the numerical implementation of the Hill-model in the solvers; if the contraction velocity is not filtered hard enough, it will switch between negative and positive contraction velocity rapidly. This leads to a discontinuous change in the contractile force, as the slope of the force-velocity relation in the Hill-model, Figure 3, is steep. In the present work, this was solved by adjusting the density of the muscle elements, so that a small mass in the order of 0.001 kg was added to each node to which a Hill-element was attached. A better solution would be to improve the numerical implementation of the Hill-models in the FE solvers to avoid too fast switching of the sign of the muscle contraction velocity.

### 6.1.2 Validation and Application

The AHBM was validated for upper body kinematics resulting from longitudinal vehicle acceleration loads for six conditions. First, the model was utilized to capture the response of front seat passengers to a 1.4 s deceleration pulse with peak amplitude of  $6.7 \text{ m/s}^2$  (Paper II). Head and sternum forward displacements were within volunteer corridors of one standard deviation width, while the sternum showed a downward movement due to the lack of intra-abdominal pressure in the HBM. Second,  $11 \text{ m/s}^2$  autonomous braking deceleration over 1.6 s was applied, with the AHBM in both the driver and passenger seats, with a standard and a reversible pre-tensioned seat belt (Paper V). Just as in the previous study, the model was once more within the one standard deviation corridors of corresponding volunteer test data, with the exception of excessive head rotations. The muscle activation levels of the AHBM were also compared with the average MVC normalized EMG from volunteers; it was found that in general the muscle activation levels of the AHBM were somewhat higher than for the volunteers (Paper V). Furthermore, the AHBM response curves were compared with the volunteer average curves, using the Weighted Integrated Factor method (Hovenga *et al.* 2005) and were found to match the average volunteer data just as well as the individual volunteers. Finally, the AHBM kinematics and muscle activations were validated for  $11 \text{ m/s}^2$  driver braking, in which the feedback control loop was complemented with a feed forward anticipatory postural response (Paper VI).

The model was applied in a parameter study to investigate the effect of variation in the activation timing and the force level of reversible pre-tensioned restraints (Paper V). It was found that stronger belt pre-tension systematically led to reduced forward head and sternum displacement caused by the braking deceleration. The largest effect was found when 570 N was activated 0.15 s before deceleration onset, causing peak head forward displacements 60 mm and 75 mm (compared with 153 mm and 232 mm without belt pre-tension) for drivers and passengers, respectively. Moreover, it was found that belt pre-tension helps to restrain the chest of the occupant, but that even 570 N was not enough to reposition the model rearward relative to its initial posture when  $11 \text{ m/s}^2$  deceleration was present.

The AHBM has the potential to be useful in further investigations of integrated systems that act on the occupant in the sagittal plane, in particular pre-crash activated restraints and varying deceleration loads. As the modeled muscle responses to both autonomous and driver brake interventions are proportional to the applied load, the model has predictive capabilities for varying load levels. However, the AHBM represents only postural feedback muscle responses; completely novel integrated systems will also have to be investigated through volunteer testing to determine whether non-linearities such as startle responses, found in Papers III and IV, are likely.

## 6.2 Car Occupant Muscle Responses

The choice of a test vehicle for the volunteer study (Papers III and IV), in contrast to the most common method of a sled setup in a laboratory, has both advantages and disadvantages. Some challenges arise, such as limitations on what type of kinematic data can be acquired, *e.g.* the legs of the driver are obscured from most angles, while on the other hand the benefit is that the setup has a higher degree of external validity, *i.e.* it more closely resembles the target environment with the volunteer performing a driving or riding task on an ordinary road. In the Paper III and IV studies, it was possible to quantify the level of muscle activity in percent of maximal volunteer efforts in an actual driving and riding environment.

### 6.2.1 Autonomous Braking and Light Impacts

Early impact biomechanics studies with volunteers showed that reflexive responses were too slow to have a significant effect on load distribution and acceleration levels of body parts in light impacts, while muscle tension prior to the event did have an effect (Begeman *et al.* 1980). More recently, Beeman *et al.* (2012) compared volunteer responses with those of an ATD and PMHSs in 2.5 g and 5 g sled tests. Their general findings were similar to those of Begeman *et al.* (1980); muscle tension prior to the acceleration pulse gives a volunteer response which is stiffer than that of an ATD; relaxed subjects are more compliant than the ATD and close to a PMHS, but with less head displacement (Beeman *et al.* 2012). As summarized in Section 4, the instruction to either be relaxed or tensed prior to the acceleration pulse has also been used in the protocol of several other studies on volunteer kinematics and muscle responses to acceleration loading. A major limitation is associated with the paradigm to test human volunteers in either a pre-tensed state or relaxed state; it remains to be investigated which type of response is representative of the real world pre-crash and crash scenarios.

For instance, it is unclear how much co-contraction, *i.e.* pre-event muscle tension, is applicable to real world pre-crash scenarios. Ejima *et al.* (2009) analyzed data from 860 frontal impacts in Japan, and found that in 48% of the impacts no evasive steering or braking was done by the driver, while in 39% the driver tried to brake prior to impact. It is likely that the occupant pre-crash response in a large portion of the no-evasive-maneuver cases would be comparable to the volunteer response found in Papers III and IV, if autonomous pre-crash braking was present. In these papers, no collision threat was included, which would be representative of a driver or occupant who has not detected the upcoming collision. Antagonistic muscle activations, *i.e.* co-contractions, were found in the volunteer reflexive muscle responses, but these were of low magnitude, typically below 5% of MVC activation. When the occupant responses in these tests were modeled with the AHBM (Paper V), it was found that controller gain tuning based on sled tests with a volunteer who was instructed to be relaxed (Ejima *et al.* 2008) was suitable to capture the response of the volunteers in autonomous braking (Papers III and IV). This supports the applicability of the relaxed condition in the sled tests to the situation during autonomous braking in an actual

vehicle, for both drivers and passengers. However, when the model's response was fitted to another volunteer sled test (Ejima *et al.* 2007), in which the volunteers only had a lap belt, the AHBM response to autonomous braking interventions was too compliant (Paper II).

The instruction for volunteers to initially tense muscles is justified for studies in which the limits of human tolerance to impact is investigated, since muscle co-contraction can influence the risk of injury (Armstrong *et al.* 1968; Hendler *et al.* 1974; Begeman *et al.* 1980; Chang *et al.* 2008). Simulation of these types of tests can motivate the inclusion of high co-contraction levels in HBMs with active muscles; for example Meijer *et al.* (2012) found the best prediction of head kinematics in 15 g impacts with 50% co-contraction. In situations with pre-crash loads however, high levels of pre-event muscle tension seem to be less motivated. In all of papers about the AHBM in this thesis, co-contractions of 3–6% have been utilized together with postural feedback control to capture volunteer reflexive responses successfully.

A startle or surprise reaction was found for some volunteers in response to the pre-tension of the seat belt (Papers III and IV). This resulted in a muscle activation peak lasting approximately 0.3 s, but it was not sustained throughout the event. It would seem more relevant to investigate the magnitude of the postural reflexive responses and potential startle reflexes in future volunteer studies with autonomous pre-crash loading and integrated safety systems, rather than to compare the difference between relaxed and tensed subjects.

### **6.2.2 Driver Voluntary Braking**

For drivers who perform an emergency braking action prior to an impact, it is likely that their postural response will differ from that during autonomous braking. Hault-Dubrule *et al.* (2011) conducted fixed-base driving simulator tests. They found a bracing response in which the volunteers extend arms and legs and push rearward into the driver seat while braking and/or steering, in response to a simulated frontal collision threat. A similar response in volunteers performing rapid maximum driver braking was also found in the volunteer study in Paper III as well as by van Rooij *et al.* (2013). In the Paper III study it was found that both antagonistic and agonistic muscles were activated. A peak average antagonistic activation of 22% MVC was found for the shoulder muscles. The peak co-contractions found in the volunteer tests were applied as constant in the AHBM for the simulation of maximum driver braking (Paper VI), but this was not enough to capture the volunteer response. Nevertheless, the simulation of a hypothesized anticipatory response, in which agonistic muscle activations of the same size as those utilized by the volunteers (Paper III) was generated in the AHBM by changes of the reference signal in the feedback controllers, did.

For the muscles of the upper body, the work in this thesis shows that, although the bracing response of drivers in emergency braking contains some co-contraction, this is not more than approximately 20% of MVC muscle activation. Average male volunteer agonist muscle activations of up to 45% were found (Paper III), and up to 50% was found for the AHBM in driver braking simulations (Paper VI). These levels of muscle contraction are moderate, and it remains to be investigated whether they correlate with the instruction for volunteers to be maximally tensed prior to a sled pre-crash test in the laboratory. When testing braced volunteer's responses to pre-crash loads in the laboratory, a more relevant instruction is probably to encourage the volunteer to exert a given force with the upper and lower extremities. This is more likely to provide muscle activations similar to a driver braking in a vehicle, than the instruction to brace by maximally co-contracting all muscles.

### 6.2.3 Variations in Occupant Postural Responses

The occupant kinematic response to braking interventions varies between subjects, giving relatively wide response corridors when one standard deviation is used for the corridor width. Therefore, scaling of the data to the 50<sup>th</sup> percentile anthropometry (Schneider *et al.* 1983), using the stature and sitting height of individual volunteers was attempted (Paper III). Although the scaling reduced the amplitude of the volunteer responses, it had only negligible effects on the coefficient of variation for the response data. Furthermore, the variation between subjects was larger than that for individual subjects in repeated trials. Hence, it seems that the variation found in occupant kinematic responses is due to differences in the postural control of the volunteers rather than anthropometric variations, *i.e.* in size and weight.

For each of the papers modeling car occupant responses in this thesis, one set of controller gains was derived, by engineering judgment (Paper II) and by utilizing a meta-model (Paper V). The AHBM response was then validated with respect to average volunteer kinematic data; this was done also for muscle activation data from normalized EMG measurements (Paper V). Thus, an AHBM response resembling a 50<sup>th</sup> percentile volunteer postural response was achieved. The feedback control method is easy to adapt to different conditions by changing the controller gains; for example it was shown that changing controller gains can capture a number of different instructions to the volunteers (Paper I). A more compliant occupant response, which would be characterized by larger displacements and larger restraint interaction forces can easily be achieved for the AHBM in Papers II and V by lowering the controller gains, in particular the proportional gain which, in principle, works as a spring.

A less compliant response of the model, is on the other hand more difficult to achieve, as increasing the controller gains reduces the stability margin of the closed-loop system. The head angle controller for the AHBM shows an oscillatory response (Paper II and V), indicating that the closed-loop system is very close to becoming unstable, *i.e.* no longer providing an undisturbed response  $y(t)$  approaching zero as time approaches infinity. In the Paper VI study, higher co-contractions were applied which remedied

this; this was probably because pre-tensioned muscles provide a damping force that increases the stability margin of the closed-loop system. Therefore, to model the response of occupants who are less compliant than the average with closed-loop postural control, a time varying co-contraction reflex such as suggested by Meijer *et al.* (2012), may be necessary. One can speculate that less compliant occupants utilize higher co-contraction levels, which will provide both an immediate damping response and allow for higher postural feedback gains.

### **6.3 Limitations and Future Work**

The present work has been limited to studying the car occupant muscle response to pre-crash braking. Further development of the AHBM should also focus on including postural control in the lateral direction in combination with the sagittal plane control presented here. Due to the asymmetry of the human body in the coronal plane, this will require a more refined muscle activation strategy; coronal and sagittal control must also be coordinated, as most muscles of the spine affect both degrees of freedom. Moreover, the AHBM has only been validated in pre-crash loading conditions. For simulation of combined pre-crash and in-crash scenarios, further development work will be required to ensure the numerical stability and validity of the model for both high level and low level loads.

The finding that voluntary driver maneuvers exhibit a postural response different from that of autonomously induced maneuvers will be useful for the modeling of evasive steering. At present, it can usually be expected that emergency avoidance by steering will be carried out by the driver, and modeling this is likely to require the inclusion of an anticipatory postural response. However, collision avoidance by autonomous steering is an integrated safety technology currently being developed (*e.g.* Eidehall *et al.* 2007). The method to model car occupant muscle responses developed in this thesis could also be applied to these types of events.

Furthermore, volunteer tests in a moving platform driving simulator, combining driver initiated and autonomous braking and steering maneuvers, with EMG instrumentation similar to that used in the studies in Papers III and IV, would allow confirmation of the hypothesis that driver anticipatory responses are present in driver initiated voluntary events but not in autonomous events.

For the study of reversible pre-tensioned seat belts, the influence on occupant muscle responses in lateral maneuvers remains to be investigated in volunteer tests. Moreover, several other factors influencing restraint performance should be investigated in future studies, for example the effect of non-optimal belt fit due to bulky clothing, and for obese occupants, or varying out-of-position conditions. For many of these conditions the AHBM developed is a suitable tool to use.

Preliminary investigations have shown that converting the AHBM to standard LS-DYNA input should be possible (Andersson 2013). This would improve the

dissemination of the AHBM to the automotive industry and facilitate using the model for the development of integrated safety systems, to improve future vehicle safety.

## 7 Conclusions

In this thesis muscle responses of car occupants subject to pre-crash braking scenarios were investigated. A human body model with active muscles (AHBM), that can model the muscle and kinematic response of car drivers and front-seat passengers in pre-crash braking scenarios, was developed; it was validated in both the driver and passenger seats. Volunteer tests to provide validation data for the AHBM were conducted, analyzed, and used. In the analysis and modeling of the volunteer tests, it was found that driver initiated braking and autonomous braking generate two different sets of postural muscle responses. The car occupant response to autonomous braking can be modeled with postural feedback control, in which stabilizing muscle activations are generated in response to external perturbations. Modeling driver initiated braking requires the inclusion of an anticipatory feed-forward response. It is hypothesized that, based on their previous experience of braking, the nervous system of car drivers generates corrective postural muscle activations proportional to the deceleration load.

Furthermore, car occupant muscle activation levels during normal driving and in braking events have been quantified in percent of maximum voluntary efforts. Moderate levels of muscle activity were found during steady-state braking for both male and female car occupants, in both agonist and antagonist muscles, indicating a co-contraction response. It was found that seat belt pre-tension can cause a startle response in the form of a bilateral, simultaneous, short peak contraction of all upper body muscles in some car occupants.

When the AHBM developed was validated in simulations of autonomous and driver braking, it was able to capture the kinematic response of the volunteers with muscle activation levels of similar magnitude. The AHBM was employed in a parameter study of the force and activation timing of reversible pre-tensioned restraints; it was predicted that, for 570 N of pre-tension, up to a 75% decrease in forward head displacement caused by the braking decelerations was possible.

The method presented, with feedback control to model occupant postural and reflexive muscle responses in FE HBM, has the potential to improve the model response in all pre-crash and in-crash scenarios, in which the effect of muscle contraction on occupant kinematics is not negligible, for example multiple events and roll-over accidents. It is a step towards the virtual development of advanced integrated restraints which can lead to improved vehicle safety and reduce the number of fatalities and injuries in the road traffic environment.



## 8 References

- Almeida J, Fraga F, Silva M, Silva-Carvalho L (2009) Feedback Control of the Head-Neck Complex for Nonimpact Scenarios using Multibody Dynamics. *Multibody System Dynamics* 21:395–416.
- Altair (2013) Altair RADIOSS – The Standard behind Structure Safety, [http://www.altairhyperworks.com/pdfs/product\\_brochures/HW\\_RADIOSS\\_Web.pdf](http://www.altairhyperworks.com/pdfs/product_brochures/HW_RADIOSS_Web.pdf), accessed 19<sup>th</sup> August 2013.
- Andersson S (2013) *Active Muscle Control in Human Body Model Simulations: Implementation of a Feedback Control Algorithm with Standard Keywords in LS-DYNA*. M.Sc. Thesis; Chalmers University of Technology, Gothenburg, Sweden.
- Antona J, Ejima S, Zama Y (2010) Influence of the Driver Conditions on the Injury Outcome in Front Impact Collisions. *Proceedings of the JSAE Conference*; Tokyo, Japan.
- Aparicio F (2005) EEVC WG19 Activities on Primary and Secondary Safety Interaction. *Proceedings of the 19<sup>th</sup> ESV Conference*; Washington, D.C., USA.
- Arbogast KB, Balasubramanian S, Seacrist T, Maltese MR, García-España JF, Hopely T, Constans E, Lopez-Valdes FK, Kent RW, Tanji H, Higuchi K (2009) Comparison of Kinematic Responses of the Head and Spine for Children and Adults in Low-Speed Frontal Sled Tests. *Stapp Car Crash Journal* 53:329–372.
- Armstrong RW, Waters HP, Stapp JP (1968) Human Muscular Restraint during Sled Deceleration. *Proceedings of the 12<sup>th</sup> Stapp Car Crash Conference*; Detroit, MI, USA.
- Bae TS, Loan P, Choi K, Hong D, Seong Mun M (2010) Estimation of Muscle Reponse using Three-Dimensional Musculoskeletal Models before Impact Situation: A Simulation Study. *Journal of Biomechanical Engineering* 132:121011-1–6.
- Barin K (1989) Evaluation of a Generalized Model of Human Postural Dynamics and Control in the Sagittal Plane. *Biological Cybernetics* 61:37–50.
- Beeman SM, Kemper AR, Madigan ML, Duma, SM (2011) Effects of Bracing on Human Kinematics in Low-Speed Frontal Sled Tests. *Annals of Biomedical Engineering* 39(12):2998–3010.
- Beeman SM, Kemper AR, Madigan ML, Franck CT, Loftus SC (2012) Occupant Kinematics in Low-speed Frontal Sled Tests: Human Volunteers, Hybrid III ATD, and PMHS. *Accident Analysis and Prevention* 47:128–139.
- Begeman PC, King AI, Levine RS, Viano DC (1980) Biodynamic Response of the Musculoskeletal System to Impact Acceleration. *Proceedings of the 24<sup>th</sup> Stapp Car Crash Conference*; Troy, MI, USA.
- Behr M, Arnoux PJ, Serre T, Thollon L, Brunet C (2006) Tonic Finite Element Model of the Lower Limb. *Journal of Biomechanical Engineering* 128:223–228.
- Behr M, Poumarat G, Serre T, Arnoux P-J, Thollon L, Brunet C (2010) Posture and Muscular Behavior in Emergency Braking: An Experimental Approach. *Accident Analysis and Prevention* 42:797–801.

- Benvenuti F, Stanhope SJ, Thomas SL, Panzer VP, Hallet M (1997) Flexibility of Anticipatory Postural Adjustments Revealed by Self-Paced and Reaction-Time Arm Movements. *Brain Research* 761:59–70.
- Berg WP, Strang AJ (2012) The Role of Electromyography (EMG) in the Study of Anticipatory Postural Adjustments, In: Steele C (ed.) *Applications of EMG in Clinical and Sports Medicine*, InTech Europe, Rijeka, Croatia.
- Blouin JS, Descarreaux M, Bélanger-Gravel A, Simoneau M, Teasdale N (2003) Attenuation of Human Neck Muscle Activity Following Repeated Imposed Trunk-Forward Linear Acceleration. *Experimental Brain Research* 150:458–464.
- Bohlin N (1967) A Statistical Analysis of 28,000 Accident Cases with Emphasis on Occupant Restraint Value. *Proceedings of the 11<sup>th</sup> Stapp Car Crash Conference*; Anaheim, CA, USA.
- Bose D, Crandall JR (2008) Influence of Active Muscle Contribution on the Injury Response of Restrained Car Occupants. *Proceedings of the Annals of Advances in Automotive Medicine Conference*.
- Bose D, Crandall JR, Untaroiu CD, Maslen EH (2010) Influence of Pre-Collision Occupant Parameters on Injury Outcome in a Frontal Collision. *Accident Analysis and Prevention* 42:1398–1407.
- Brault JR, Siegmund GP, Wheeler JB (2000) Cervical Muscle Response during Whiplash: Evidence of a Lengthening Muscle Contraction. *Clinical Biomechanics* 15:426–435.
- Brolin K, Halldin P, Leijonhufvud I (2005) The Effect of Muscle Activation on Neck Response. *Traffic Injury Prevention* 6:67–76.
- Brolin K, Hedenstierna S, Halldin P, Bass C, Alem N (2008) The Importance of Muscle Tension on the Outcome of Impacts with a Major Vertical Component. *International Journal of Crashworthiness* 13(5):487–498.
- Budziszewski P, van Nunen E, Mordaka JK, Kędzior K (2008) Active Controlled Muscles in Numerical Model of Human Arm for Movement in Two Degrees of Freedom. *Proceedings of the IRCOBI Conference*; Bern, Switzerland.
- Cappon H, Mordaka J, van Rooij L, Adamec J, Praxl N, Muggenthaler H (2007) A Computational Human Model with Stabilizing Spine: A Step Towards Active Safety. SAE Technical Paper No. 2007-01-1171; SAE International. Warrendale, PA, USA.
- Carlsson S and Davidsson J (2011) Volunteer Occupant Kinematics during Driver Initiated and Autonomous Braking when Driving in Real Traffic Environments. *Proceedings of the IRCOBI Conference*; Krakow, Poland.
- Chancey VC, Nightingale RW, Van Ee CA, Knaub KE, Myers BS (2003) Improved Estimation of Human Neck Tensile Tolerance: Reducing the Range of Reported Tolerance using Anthropometrically Correct Muscles and Optimized Physiologic Initial Conditions. *Stapp Car Crash Journal* 47:135–153.
- Chang CY, Rupp JD, Kikuchi N, Schneider LW (2008) Development of a Finite Element Model to Study the Effects of Muscle Forces on Knee-Thigh-Hip Injuries in Frontal Crashes. *Stapp Car Crash Journal* 52:475–504.

- Chang CY, Rupp JD, Kikuchi N, Schneider LW (2009) Predicting the Effects of Muscle Activation on Knee, Thigh, and Hip Injuries in Frontal Crashes Using a Finite-Element Model with Muscle Forces from Subject Testing and Musculoskeletal Modeling. *Stapp Car Crash Journal* 53:291–328.
- Choi HY, Sah SJ, Lee B, Cho HS, Kang SJ, Mun MS, Lee I, Lee J (2005) Experimental and Numerical Studies of Muscular Activations of Bracing Occupant. *Proceedings of the 19<sup>th</sup> ESV Conference*; Washington, D.C., USA.
- Coelingh E, Jakobsson L, Lind H, Lindman M (2007) Collision Warning with Auto Brake – A Real-life Safety Perspective. *Proceedings of the 20<sup>th</sup> ESV Conference*; Lyon, France.
- Cummings P, Wells JD, Rivara FP (2003) Estimating Seat Belt Effectiveness using Matched-pair Cohort Methods. *Accident Analysis and Prevention* 35:143–149.
- de Jager MKJ (1996) *Mathematical Head-Neck Models for Acceleration Impacts*. Ph.D. Thesis; Eindhoven University of Technology, Eindhoven, the Netherlands.
- de Vlugt E (2004) *Identification of Spinal Reflexes*. Ph.D. Thesis: Delft University of Technology, Delft, The Netherlands.
- de Vlugt E, Schouten AC, van der Helm FCT (2002) Adaptation of Reflexive Feedback during Arm Posture to Different Environments. *Biological Cybernetics* 87:10–26.
- de Vlugt E, Schouten AC, van der Helm FCT (2006) Quantification of Intrinsic and Reflexive Properties during Multijoint Arm Posture. *Journal of Neuroscience Methods* 155:328–349.
- de Wolf S, Slijper H, Latash ML (1998) Anticipatory Postural Adjustments during Self-Paced and Reaction-Time Movements. *Experimental Brain Research* 121:7–19.
- Deng YC, Goldsmith W (1987) Response of a Human Head/Neck/Upper-Torso Replica to Dynamic Loading – II. Analytical/Numerical Model. *Journal of Biomechanics* 20(5):487–497.
- Develet J-A, Carlsson A, Svensson M, Fredriksson R, Bråse D, Holcombe S (2013) Evaluation of the Biofidelity of the BioRID-II and THOR-NT Anthropometric Test Devices under Seatbelt Pre-Pretensioner Loading in Stationary Conditions. *Proceedings of the Ohio State University Injury Biomechanics Seminar*; Columbus, OH, USA.
- Dibb AT, Cox CA, Nightingale RW, Luck JF, Cutcliffe HC, Myers BS, Arbogast KB, Seacrist T, Bass CR (2013) Importance of Muscle Activations for Biofidelic Pediatric Neck Response in Computational Models. *Traffic Injury Prevention* 14(Sup1):S116–S127.
- Distner M, Bengtsson M, Broberg T, Jakobsson L (2009) City Safety – A System Addressing Rear-End Collisions at Low Speeds. *Proceedings of the 21<sup>st</sup> ESV Conference*; Stuttgart, Germany.
- Eidehall A, Pohl J, Gustafsson F, Ekmark J (2007) Toward Autonomous Collision Avoidance by Steering. *IEEE Transactions on Intelligent Transportation Systems* 8(1):84–94.

- Ejima S, Ito D, Satou F, Mikami K, Ono K, Kaneoka K, Shiina I (2012) Effects of Pre-Impact Swerving/Steering on Physical Motion of the Volunteer in the Low-Speed Side-Impact Sled Test. *Proceedings of the IRCOBI Conference*; Dublin, Republic of Ireland.
- Ejima S, Ono K, Holcombe S, Kaneoka K, Fukushima M (2007) A Study on Occupant Kinematics Behaviour and Muscle Activities during Pre-Impact Braking based on Volunteer Tests. *Proceedings of the IRCOBI Conference*; Maastricht, the Netherlands.
- Ejima S, Ono K, Kaneoka K, Fukushima M (2005) Development and Validation of the Human Neck Muscle Model under Impact Loading. *Proceedings of the IRCOBI Conference*; Prague, Czech Republic.
- Ejima S, Zama Y, Ono K, Kaneoka K, Shiina I, Asada H (2009) Prediction of Pre-Impact Occupant Kinematic behavior Based on the Muscle Activity during Frontal Collision. *Proceedings of the 21<sup>st</sup> ESV Conference*; Stuttgart, Germany.
- Ejima S, Zama Y, Satou F, Holcombe S, Ono K, Kaneoka K, Shiina I (2008) Prediction of the Physical Motion of the Human Body based on Muscle Activity during Pre-Impact Braking. *Proceedings of the IRCOBI Conference*; Bern, Switzerland.
- Erhart T (2010) An Overview of User Defined Interfaces in LS-DYNA. Paper presented at the LS-DYNA Forum; Bamberg, Germany.
- ESI (2013) Crash, Impact & Safety – PAM-CRASH, <http://www.esi-group.com/products/crash-impact-safety/pam-crash>, accessed 19<sup>th</sup> August 2013.
- European Commission (2012) *EU Transport in figures 2012*. Publications Office of the European Union, Luxembourg.
- European Commission (2013) Road Safety Evolution in the EU, [ec.europa.eu/transport/road\\_safety/specialist/statistics/index\\_en.htm](http://ec.europa.eu/transport/road_safety/specialist/statistics/index_en.htm), accessed 6<sup>th</sup> February 2014.
- Fraga F, van Rooj L, Symeonidis I, Peldschus S, Happee R, Wismans J (2009) Development and Preliminary Validation of a Motorcycle Rider Model with Focus on Head and Neck Biofidelity, Recurring to Line Element Muscle Models and Feedback Control. *Proceedings of the 21<sup>st</sup> ESV Conference*; Stuttgart, Germany.
- Gerdes VGJ, Happee R (1994) The Use of an Internal Representation in Fast Goal-Directed Movements: A Modeling Approach. *Biological Cybernetics* 70:513–524.
- Good CA, Viano DC, Ronsky JL (2008a) Biomechanics of Volunteers Subject to Loading by a Motorized Shoulder Belt Tensioner. *Spine* 33:E225–E235.
- Good CA, Viano DC, Ronsky JL (2008b) The Hybrid III Dummy Family Subject to Loading by a Motorized Shoulder Belt Tensioner. *SAE International Journal of Passenger Cars-Mechanical Systems* 1(1):383–395.
- Happee R, Hoofman M, van den Kroonenberg AJ, Morsink P, Wismans J (1998) A Mathematical Human Body Model for Frontal and Rearward Seated

- Automotive Impact Loading. *Proceedings of the 42<sup>nd</sup> Stapp Car Crash Conference*; Tempe, Arizona, USA.
- Hault-Dubrulle A, Robach F, Pacaux M-P, Morvan, H (2011) Determination of Pre-Impact Occupant Postures and Analysis of Consequences on Injury Outcome. Part I: A Driving Simulator Study. *Accident Analysis and Prevention* 43:66–74.
- Hedenstierna S (2008) *3D Finite Element Modeling of Cervical Musculature and its Effect on Neck Injury Prevention*. Ph.D. Thesis; Royal Institute of Technology, Stockholm, Sweden.
- Hedenstierna S, Halldin P, Brodin K (2008) Evaluation of a Combination of Continuum and Truss Finite Elements in a Model of Passive and Active Muscle Tissue. *Computer Methods in Biomechanics and Biomedical Engineering* 11(6):627–639.
- Hell W, Schick S, Langweider K, Zellmer H (2002) Biomechanics of the Cervical Spine Injuries in Rear End Car Impacts: Influence of Car Seats and Possible Evaluation Criteria. *Traffic Injury Prevention* 3:127–140.
- Hendler E, O'Rourke J, Schulman M, Katzeff M, Domzalski L, Rodgers S (1974) Effect of Head and Body Position and Muscular Tensing on Response to Impact. *Proceedings of the 18<sup>th</sup> Stapp Car Crash Conference*; Ann Arbor, Michigan, USA.
- Hetier M, Wang X, Robache F, Autuori B, Morvan H (2005) Experimental Investigation and Modeling of Driver's Frontal Pre-crash Postural Anticipation. *Proceedings of the Digital Human Modeling for Design and Engineering Symposium*; Iowa City, Iowa, USA.
- Hill AV (1938) The Heat of Shortening and the Dynamic Constants of Muscle. *Proceedings of the Royal Society* B126:136–195.
- Hill AV (1970) *The First and Last Experiments in Muscle Mechanics*. University Press, Cambridge, UK.
- Hodges PW (1999) Is there a Role for Transversus Abdominis in Lumbo-Pelvic Stability? *Manual Therapy* 4(2):74–86.
- Hovenga PE, Spit HH, Uijldert M, Dalenoort AM (2005) Improved Prediction of Hybrid-III Injury Values using Advanced Multibody techniques and Objective Rating. *Proceedings of the SAE World Congress*; Detroit, MI.
- Huber P, Christova M, D'Addetta GA, Gallasch E, Kirschbichler S, Mayer C, Prügler A, Rieser A, Sinz W, Wallner D (2013) Muscle Activation Onset Latencies and Amplitudes during Lane Change in a Full Vehicle Test. *Proceedings of the IRCOBI Conference*; Gothenburg, Sweden.
- Huxley AF (1957) Muscle Structure and Theories of Contraction. *Progress in Biophysics and Biophysical Chemistry* 7:255–318.
- IRCOBI (2006) Future Research Directions in Injury Biomechanics and Passive Safety Research. [http://www.ircobi.org/downloads/future\\_research.pdf](http://www.ircobi.org/downloads/future_research.pdf), Accessed 19<sup>th</sup> December 2013.
- Ito D, Ejima S, Kitajima S, Katoh R, Ito H, Sakane M, Nishino T, Nakayama K, Ato T, Kimura T (2013) Occupant Kinematic Behavior and Effects of a Motorized

- Seatbelt on Occupant Restraint of Human Volunteers during Low Speed Frontal Impact: Mini-sled Tests with Mass Production Car Seat. *Proceedings of the IRCOBI Conference*; Gothenburg, Sweden.
- Iwamoto M, Kisanuki Y, Watanabe I, Furusu K, Miki K (2002) Development of a Finite Element Model of the Total Human Model for Safety (THUMS) and Application to Injury Reconstruction. *Proceedings of the IRCOBI Conference*; Munich, Germany.
- Iwamoto M, Nakahira Y, Kimpara H, Sugiyama T (2009) Development of a Human FE Model with 3-D Geometry of Muscles and Lateral Impact Analysis for the Arm with Muscle Activity. SAE Technical Paper No. 2009-01-226; Society of Automotive Engineers, Warrendale, PA, USA.
- Iwamoto M, Nakahira Y, Kimpara H, Sugiyama T (2012) Development of a Human Body Finite Element Model with Multiple Muscles and their Controller for Estimating Occupant Motions and Impact Responses in Frontal Crash Situations. *Stapp Car Crash Journal* 56:231-268.
- Iwamoto M, Nakahira Y, Sugiyama T (2011) Investigation of Pre-impact Bracing Effects for Injury Outcome using an Active Human FE Model with 3D Geometry of Muscles. *Proceedings of the 22<sup>nd</sup> ESV Conference*; Washington, D.C., USA.
- Jost R, Nurick GN (2000) Development of a Finite Element Model of the Human Neck Subjected to High g-Level Lateral Deceleration. *International Journal of Crashworthiness* 5(3):259-270.
- Kawato M (1999) Internal Models for Motor Control and Trajectory Planning. *Current Opinion in Neurobiology* 9:718-727.
- Khodaei H, Mostofizadeh S, Brodin K, Johansson H, Östh J (2013) Simulation of Active Skeletal Muscle Tissue with a Transversely Isotropic Viscohyperelastic Continuum Material Model. *Journal of Engineering in Medicine* 227(5):571-580.
- Kullgren A, Eriksson L, Boström O, Krafft M (2003) Validation of Neck Injury Criteria using Reconstructed Real-Life Rear-End Crashes with Recorded Crash Pulses. *Proceedings of the 18<sup>th</sup> ESV Conference*; Nagoya, Japan.
- Lie A, Strandroth J, Tingvall C (2013) Government Status Report, Sweden 2013. *Proceedings of the 23<sup>rd</sup> ESV Conference*; Seoul, South Korea.
- Lie A, Tingvall C, Krafft M, Kullgren A (2006) The Effectiveness of Electronic Stability Control (ESC) in Reducing Real Life Crashes and Injuries. *Traffic Injury Prevention* 7:38-43.
- LSTC (2013) *LS-DYNA User's Manual Volume I Version 971 R6.1.0*. Livermore Software Technology, Livermore, CA, USA.
- Mages M, Seyffert M, Class U (2011) Analysis of the Pre-Crash Benefit of Reversible Belt Pre-pretensioning in Different Accident Scenarios. *Proceedings of the 22<sup>nd</sup> ESV Conference*; Washington, D.C., USA.
- Magnusson ML, Pope MH, Hasselquist L, Bolte KM, Ross M, Goel VK, Lee JS, Spratt K, Clark CR, Wilder DG (1999) Cervical Electromyographic Activity during Low-Speed Rear Impact. *European Spine Journal* 8:118-125.

- Marieb EN, Hoehn K, (eds.) (2010) *Human Anatomy and Physiology*, 8th edn. Pearson Benjamin Cummings, San Francisco, CA, USA.
- Massion J (1992) Movement, Posture and Equilibrium: Interaction and Coordination. *Progress in Neurobiology* 38:35–56.
- Meijer R, Broos J, Elrofai H, de Bruijn E, Forbes P, Happee R (2013a) Modelling of Bracing in a Multi-Body Active Human Model. *Proceedings of the IRCOBI Conference*; Gothenburg, Sweden.
- Meijer R, Elrofai H, Broos J, van Hassel E (2013b) Evaluation of an Active Multi-Body Human Model for Braking and Frontal Crash Events. *Proceedings of the 23<sup>rd</sup> ESV Conference*; Seoul, South Korea.
- Meijer R, Rodarius C, Adamec J, van Nunen E, van Rooij L (2008) A First Step in Computer Modelling of the Active Human Response in a Far-side Impact. *International Journal of Crashworthiness* 13(6):643–652.
- Meijer R, van Hassel E, Broos J, Elrofai H, van Rooij L, van Hooijdonk P (2012) Development of a Multi-Body Human Model that Predicts Active and Passive Human Behavior. *Proceedings of the IRCOBI Conference*; Dublin, Republic of Ireland.
- Morris R and Cross G (2005) Improved Understanding of Passenger Behaviour during Pre-Impact Events to Aid Smart Restraint Development. *Proceedings of the 19<sup>th</sup> ESV Conference*; Washington, D.C., USA.
- Muggenthaler H, Adamec J, Praxl N, Schönplflug M (2005) The Influence of Muscle Activity on Occupant Kinematics. *Proceedings of the IRCOBI Conference*; Prague, Czech Republic.
- Nemirovsky N, van Rooij L (2010) A New Methodology for Biofidelic Head-Neck Postural Control. *Proceedings of the IRCOBI Conference*; Hannover, Germany.
- NHTSA (2012) Traffic Safety Facts 2011. US Department of Transportation, Washington, D.C., DOT HS 811 754.
- Norin H, Carlsson G, Korner J (1984) Seat Belt Usage in Sweden and Its Injury Reducing Effect. SAE Technical Paper No. 840194. Society of Automotive Engineers, Warrendale, PA.
- Ono K, Kaneoka K, Wittek A, Kajzer J (1997) Cervical Injury Mechanism Based on the Analysis of Human Cervical Vertebral Motion and Head-Neck-Torso Kinematics during Low Speed Rear Impacts. *Proceedings of the 41<sup>st</sup> Stapp Car Crash Conference*; Lake Buena Vista, Florida, USA.
- Park G, Kim T, Crandall JR, Arregui-Dalmases C, Luzon-Narro J (2013) Comparison of Kinematics of GHBMC to PMHS on the Side Impact Condition. *Proceedings of the IRCOBI Conference*; Gothenburg, Sweden.
- Prasad P, Chou CC (2002) A Review of Mathematical Occupant Simulation Models, in Nahum AM and Melvin JW (eds.) *Accidental Injury*, 2<sup>nd</sup> edn., Springer Science+Business Media, New York, USA.
- Prügler A, Huber P, Rieser A, Steiner K, Kirschbichler S, Eichberger A (2011) Implementation of Reactive Human Behavior in a Numerical Human Body

- Model using Controlled Beam Elements as Muscle Element Substitutes. *Proceedings of the 22<sup>nd</sup> ESV Conference*; Washington, D.C., USA.
- Robin S (2001) Humos: Human Model for Safety – A Joint Effort Towards the Development of Refined Human-like Car Occupant Models. *Proceedings of the 17<sup>th</sup> ESV Conference*; Amsterdam, the Netherlands.
- Schittenhelm H (2009) The Vision of Accident Free Driving – How Efficient are We Actually in Avoiding or Mitigating Longitudinal Real World Accidents. *Proceedings of the 21<sup>st</sup> ESV Conference*; Stuttgart, Germany.
- Schneider LW, Robbins DH, Pflug MA, Snyder RG (1983) Development of Anthropometrically based Design Specifications for an Advanced Adult Anthropomorphic Dummy Family, Vol. 1, National Highway Traffic Safety Administration Report No. UMTR 1-83-53-1, Washington, D.C., USA.
- Schöneburg R, Baumann K-H, and Fehring M (2011) The Efficiency of PRE-SAFE® Systems in Pre-braked Frontal Collision Situations. *Proceedings of the 22<sup>nd</sup> ESV Conference*; Washington, D.C., USA.
- Seiffert U, Gonter M (2014) *Integrated Automotive Safety Handbook*. SAE International, Warrendale, Pennsylvania, USA.
- Shugar TA (1975) Transient Structural Response of the Linear Skull-Brain System. *Proceedings of the 19<sup>th</sup> Stapp Car Crash Conference*; San Diego, California, USA.
- Siegmund GP, Sanderson DJ, Inglis JT (2004) Gradation of Neck Muscle Responses and Head/Neck Kinematics to Acceleration and Speed Change in Rear-End Collisions. *Stapp Car Crash Journal* 48:419–430.
- Siegmund GP, Sanderson DJ, Myers BS, Inglis JT (2003a) Awareness Affects the Response of Human Subjects Exposed to a Single Whiplash-Like Perturbation. *Spine* 28(7):671–679.
- Siegmund GP, Sanderson DJ, Myers BS, Inglis JT (2003b) Rapid Neck Muscle Adaptation Alters the Head Kinematics of Aware and Unaware Subjects Undergoing Multiple Whiplash-like Perturbations. *Journal of Biomechanics* 36:473–482.
- Sugiyama T, Kimpara H, Iwamoto M, Yamada D, Nakahira Y, Masatoshi H (2007) Effects of Muscle Tense on Impact Responses of Lower Extremity. *Proceedings of the IRCOBI Conference*; Maastricht, the Netherlands.
- Szabo TJ, Welcher JB (1996) Human Subject Kinematics and Electromyographic Activity during Low Speed Rear Impacts. *Proceedings of the 40<sup>th</sup> Stapp Car Crash Conference*; Albuquerque, New Mexico, USA.
- TASS (2013) MADYMO Solver: <https://www.tassinternational.com/madymo-solver>, accessed 19<sup>th</sup> August 2013.
- Tobata H, Takagi H, Pal C, Fukuda S (2003) Development of Pre-Crash Active Seatbelt System for Real World Safety. *Proceedings of the 18<sup>th</sup> ESV Conference*; Nagoya, Japan.

- Toyota (2008) *Users' Guide of Computational Human Model THUMS® – AM50 Occupant Model: Version 3.0–080225*. Toyota Motor Corporation, Toyota Central Labs Inc, Toyota City, Aichi, Japan.
- Toyota (2011) *Documentation – Total Human Model for Safety (THUMS) AM50 Pedestrian/Occupant model*. Toyota Motor Corporation, Toyota City, Aichi, Japan.
- van den Bogert AJ, Gerritsen KGM, Cole GK (1998) Human Muscle Modeling from a User's Perspective. *Journal of Electromyography and Kinesiology* 8:119–124.
- van der Horst M (2002) *Human Head Neck Response in Frontal, Lateral and Rear End Impact Loading – Modeling and Validation*. Ph.D. Thesis; Eindhoven University of Technology, Eindhoven, the Netherlands.
- van Rooij L (2011) Effect of Various Pre-Crash Braking Strategies on Simulated Human Kinematic Response with Varying Levels of Driver Attention. *Proceedings of the 22<sup>nd</sup> ESV Conference*; Washington, D.C., USA.
- van Rooij L, Pauwelussen J, Op den Camp O, Janssen R (2013) Driver Head Displacement during (Automatic) Vehicle Braking Tests with Varying Levels of Distraction. *Proceedings of the 23<sup>rd</sup> ESV Conference*; Seoul, Republic of Korea.
- Ward CC, Thompson RB (1975) The Development of a Detailed Finite Element Brain Model. *Proceedings of the 19<sup>th</sup> Stapp Car Crash Conference*; San Diego, California, USA.
- WHO (2013) *European Facts and Global Status Report on Road Safety 2013*. World Health Organization, Regional Office for Europe, Copenhagen, Denmark.
- Wikimedia (2013) [http://commons.wikimedia.org/wiki/File:Illu\\_muscle\\_structure.jpg](http://commons.wikimedia.org/wiki/File:Illu_muscle_structure.jpg), Accessed 23<sup>rd</sup> August 2013.
- Winter DA (1995) Human Balance and Posture Control during Standing and Walking. *Gait & Posture* 3:193–214.
- Winter DA (2009) *Biomechanics and Motor Control of Human Movement, 4<sup>th</sup> edn*. John Wiley & Sons, Hoboken, New Jersey, USA.
- Winters JM, Stark L (1985) Analysis of Fundamental Human Movement Patterns through the Use of In-depth Antagonistic Muscle Models. *IEEE Transactions on Biomedical Engineering* 32(10):826–839.
- Wismans J, Maltha J, Melvin JW, Stalnaker RL (1979) Child Restraint Evaluation by Experimental and Mathematical Simulation. *Proceedings of the 23<sup>rd</sup> Stapp Car Crash Conference*; San Diego, CA. pp. 383–415.
- Wittek A (2000) *Mathematical Modeling of the Muscle Effects on the Human Body Responses under Transient Loads – Example of Head-Neck Complex*. Ph.D. Thesis; Chalmers University of Technology, Gothenburg, Sweden.
- Wittek A, Kajzer J (1997) Modeling the Muscle Influence on the Kinematics of the Head-Neck Complex in Impacts. *Memoirs of the School of Engineering, Nagoya University* 49:155–205.
- Woitsch G, Sinz W (2014) Influences of Pre-Crash Braking Induced Dummy – Forward Displacements on Dummy Behaviour during EuroNCAP Frontal Crashtest. *Accident Analysis and Prevention* 62:268–275.

Yang KH, Hu J, White NA, King AI (2006) Development of Numerical Models for Injury Biomechanics Research: A Review of 50 Years of Publications in the Stapp Car Crash Conference. *Stapp Car Crash Journal* 50:429–490.

## Appendix A: Implementation of the AHBM

In the AHBM the postural and reflexive responses are modeled for the trunk and upper extremities using closed-loop systems with PID controllers as shown in Figure A1, while the lower extremity muscles are open-loop controlled with pre-defined activation levels. The controllers and activation dynamics model are implemented in the solution control subroutine [7], while the musculoskeletal model is solved using the standard LS-DYNA code.

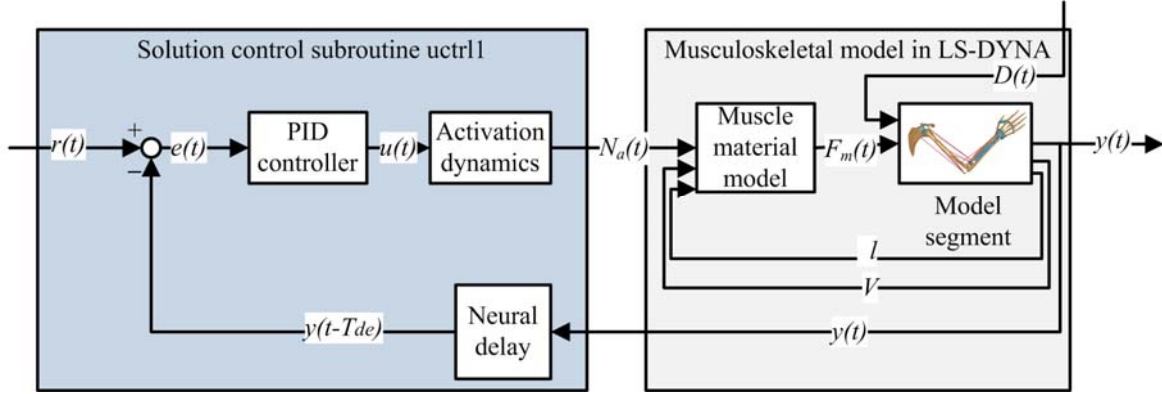


Figure A1. Schematic representation of the implementation of the AHBM.

### A.1 Notation

#### Variables

$F_m$	Muscle force
$f_v$	Force-velocity relation
$f_l$	Force-length relation
$f_{pe}$	Parallel elastic stiffness
$l$	Muscle length
$V$	Muscle shortening velocity
$v$	Normalized muscle shortening velocity
$y$	Segment angle
$r$	Reference angle
$e$	Error signal
$u$	Control signal
$u_s$	Scaled control signal
$N_e$	Neural excitation
$N_a$	Muscle activation level

#### Keyword notation

alm	Activation level
cer	Parallel elastic constant, equal to $C_{pe}$
dmp	Damping constant
mid	Material identification number
pis	Maximum isometric stress
ro	Density
sfr	Scale factor for the maximum shortening velocity as a function of muscle length
sno	Constant determining the optimal length, $l_{opt}$
srm	Constant determining the maximum shortening velocity $V_{max}$
ssm	Parallel elastic constant, equal to $PE_{max}$
ssp	Switch for the parallel elastic model
svr	Referring to a load curve with the $f_v$ function
svs	Referring to a load curve with the $f_l$ function

#### Constants

$\Delta t$	Time step
$\sigma_{max}$	Maximum isometric stress
$\sigma_d$	Parallel elastic damping stress
$C_{leng}$	$f_v$ constant, lengthening
$C_{mvl}$	$f_v$ constant, lengthening asymptote
$C_{short}$	$f_v$ constant, shortening
$C_{pe}$	Parallel elastic constant
$C_{sh}$	$f_l$ shape constant
$k_p$	Proportional gain
$k_i$	Integral gain
$k_d$	Derivative gain
$l_{initial}$	Muscle length at $t = 0$
$l_{opt}$	Optimal muscle length
$PCSA$	Physiological Cross-Sectional Area
$PE_{max}$	Parallel element strain at $\sigma_{max}$
$n$	Simulation cycle
$V_{max}$	Maximum shortening velocity
$T_{de}$	Neural delay
$T_f$	Derivative filter time constant
$T_{naa}$	Activation time constant
$T_{nad}$	Deactivation time constant
$T_{ne}$	Neural excitation time constant

## A.2 Musculoskeletal Model

For the muscles in the AHBM, a 1D phenomenological Hill-type muscle material model is utilized. The axial stress of the muscles is computed according to

$$\sigma = \left( N_a(t) \cdot f_v(v) \cdot f_l(l) + f_{pe}(l) \right) \cdot \sigma_{max} + \sigma_d \quad (\text{A1})$$

where  $N_a(t)$  is the muscle activation level and  $\sigma_{max}$  is the maximum isometric stress of the muscle. The force-velocity,  $f_v$ , and force-length,  $f_l$ , functions in Equation A1 are the Hill-equations for the contractile element, shown in Figure 3. They are modeled according to [17, 19]:

$$f_v(V) = \begin{cases} 0 & v \leq -1 \\ \frac{1+v}{1 - \frac{v}{C_{short}}} & -1 < v \leq 0 \\ \frac{1 + v \frac{C_{mvl}}{C_{leng}}}{1 + \frac{v}{C_{leng}}} & v > 0 \end{cases}, \quad v = \frac{V}{V_{max}} \quad (\text{A2})$$

$$f_l(l) = \exp\left\{-\left[\frac{\frac{l}{l_{opt}} - 1}{C_{sh}}\right]^2\right\} \quad (\text{A3})$$

where the shape of  $f_v$  is determined by three constants,  $C_i$ , and the maximum shortening velocity of the muscle,  $V_{max}$ . Here,  $C_{short}$  determines the shape for concentric shortening, while  $C_{leng}$  determines the transition between concentric shortening and eccentric lengthening of the muscle;  $C_{mvl}$  determines the asymptotic value for increasing eccentric lengthening speeds. For  $f_l$  in Equation A3, the shape parameter,  $C_{sh}$ , determines the width of the curve. The contribution of the parallel elastic stiffness,  $f_{pe}$  in Equation A1, is approximated by [17, 19]:

$$f_{pe}(l) = \left\{ \frac{1}{\exp(C_{pe}) - 1} \right\} \left\{ \exp\left[ \frac{C_{pe}}{PE_{max}} \left( \frac{l}{l_{opt}} - 1 \right) \right] - 1 \right\} \quad (\text{A4})$$

where the parameter  $PE_{max}$  represents the amount of strain when the stress of the passive element is equal to  $\sigma_{max}$ . The shape parameter  $C_{pe}$  determines the curvature of the PE stiffness, see Figure 3.

In Equation A1,  $\sigma_d$  is a damping component due to the passive properties of the muscle, modelled according to

$$\sigma_d(V) = \frac{dmp}{l_{opt}} V. \quad (\text{A5})$$

The representation of the passive muscle damping in Equation A5 was chosen due to the implementation in the LS-DYNA material keyword \*MAT\_MUSCLE [11] that was utilized in the AHBM. In tuning simulations (Paper I) to find appropriate passive damping of the elbow joint, a value for  $d_{mp}$  of 4000 Ns/m<sup>2</sup> was found. This value was used for all muscles in the AHBM; however, it produces negligible amounts of damping stress in comparison with to the contribution of the contractile element with only a few percent of activation. The structure of the \*MAT\_MUSCLE keyword in LS-DYNA is shown in Figure A2.

```
*MAT_MUSCLE
$#      mid      ro      sno      srm      pis      ssm      cer      dmp
 43511010 1.000E-10 0.950000 10.000000 1.000000 0.800000 6.150000 0.004000
$#      alm      sfr      svr      ssp
-43511018 1.000000 -43500024 -43500012 0.000
```

**Figure A2. Muscle material keyword in the LS-DYNA input deck for the AHBM, in the unit system mm–s–tonne. This sample keyword is for the left anterior deltoid muscle. Keyword notation from LS-PREPOST (LSTC Inc., Livermore, CA, USA).**

A unique material identification number,  $mid$ , is used for each muscle element. The density of the muscle material,  $ro$ , is chosen so that when multiplied by the cross sectional area of the muscle, defined on the card \*SECTION\_BEAM, a mass in the order of 0.001 kg is added to each attachment node. The parameter  $sno$  determines the optimal muscle length,  $l_{opt}$ , at which maximal isometric stress is generated, relative to the muscle length for the first time step,  $l_{initial}$ , of the simulation according to

$$l_{opt} = \frac{l_{initial}}{sno}. \quad (A6)$$

The maximum shortening velocity,  $V_{max}$  in Equation A2, is determined by the parameter  $srm$ , such that

$$V_{max} = srm \cdot l_{opt}. \quad (A7)$$

The maximum isometric stress,  $\sigma_{max}$  in Equation A1, is equal to the parameter  $pis$  in the keyword in Figure A2. The parameters  $ssm$  and  $cer$  are related to the parallel stiffness of the muscle and the material routine \*MAT\_MUSCLE utilizes the parallel stiffness function in Equation A4. Hence, the parameter  $ssm$  is equal to  $PE_{max}$ , and  $cer$  is equal to  $C_{pe}$ . The function of  $d_{mp}$  is described in Equation A5.

In the second row in Figure A2, the parameter  $ssp = 0$  indicates that the exponential function of Equation A4 should be used for the parallel elastic stiffness, while  $sfr$  is a scaling factor for the maximum shortening velocity, as a function of element length not utilized in the AHBM, and set to unity. The length and force velocity relations of the Hill-element, Equations A2 and A3, are tabulated in load curves

(\*DEFINE\_CURVE) with the normalized length,  $l/l_{opt}$ , and normalized shortening velocity,  $V/V_{max}$ , for the abscissa.

Finally, the parameter  $a_{lm}$  is the muscle activation level,  $N_a(t)$ , in Equation A1; it refers to a load curve which is defined in the input keyword deck without any other information than the load curve id, see Figure A3.

```
*DEFINE_CURVE
$#      lcid
      43511018
*DEFINE_CURVE...
```

**Figure A3. Definition of activation load curves,  $a_{lm}$ , for the muscle material model in LS-DYNA. The \*DEFINE\_CURVE keyword with only a curve id, lcid, generates a variable in the uctrl1 subroutine in the dyn21.f file.**

The definition of an “empty” load curve, Figure A3, allocates a variable space in the vector  $fval_{new}$  in the solution control subroutine, uctrl1, in the file dyn21.f which is a part of the source code of LS-DYNA [7]. For each muscle, an activation level is calculated and stored in the variable space for its corresponding  $a_{lm}$  load curve as described in subsequent sections.

### A.3 Controller Model

For the PID controllers, the segment angles,  $y(t)$ , of the elbows are calculated by using the definition of the scalar product of vectors so that

$$y_{elbows} = \cos^{-1} \left[ \frac{\mathbf{a} \cdot \mathbf{b}}{|\mathbf{a}| \cdot |\mathbf{b}|} \right] \quad (A7)$$

for vectors  $\mathbf{a}$  and  $\mathbf{b}$  spanning the length of the humeri and ulnae as shown in Figure A4. The shoulder flexion angles and the spinal segment angles are calculated in the lateral plane for the vectors,  $\mathbf{u}$ , shown as solid lines in Figure A4 so that

$$y_i = \tan^{-1} \left( \frac{u_{ix}}{u_{iz}} \right) \quad (A8)$$

for  $i = \text{head, cervical spine, lumbar spine, or humeri}$ . All segment angles are calculated relative to their value in the first time step of the simulation. Hence, a non-zero value represents a deviation from the initial posture.

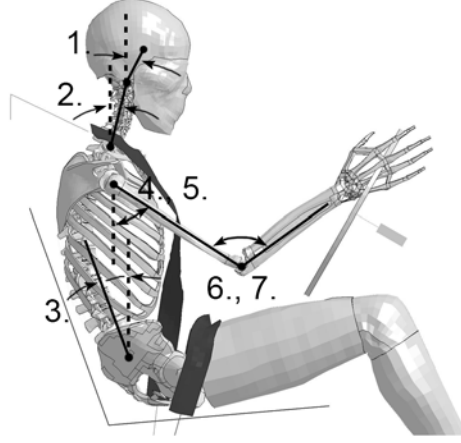


**Figure A4. PID controller angle definitions. The head (1), cervical (2), lumbar (3), and shoulder (4, 5) angle controllers all use the angle of the body part with respect to the vertical axis, while the elbow (6, 7) controllers utilize the relative angle between the corresponding humerus and ulna. Soft tissues of the trunk, neck, and upper extremities are not shown.**

In the solution control subroutine, a neural delay is implemented for the segment angles,  $y(t)$ , to represent the neural transmission time,  $T_{de}$ , required both for sensory and motor neural signals. The delayed angle signals,  $y(t-T_{de})$ , are compared with the reference angles  $r(t)$  to calculate the controller error  $e(t)$ :

$$e(t) = r(t) - y(t - T_{de}). \quad (\text{A9})$$

In simulations with the objective to maintain the initial posture (Papers I, II, and V), the references were always set to zero. In the Paper VI study, time varying reference signals,  $r(t)$ , proportional to the applied deceleration, were used to model driver anticipatory postural responses. The PID controllers are then utilized to calculate correction control signals  $u(t)$  according to:

$$u(t) = k_p \cdot e(t) + k_i \cdot \int_0^t e(\tau) d\tau + k_d \cdot \frac{de(t)}{dt}. \quad (\text{A10})$$

In Equation A10,  $k_p$ ,  $k_i$ , and  $k_d$  are the proportional, integral, and derivative gains of the PID controllers. The integral of the error is calculated using summation and the trapezoidal rule with the value of  $e(t)$  for the present,  $n$ , and previous,  $n-1$ , time step,  $\Delta t$ :

$$\int_0^{t_n} e(\tau) d\tau = ie(t_n) = ie(t_{n-1}) + \frac{e(t_n) + e(t_{n-1})}{2} \cdot \Delta t. \quad (\text{A11})$$

The derivative of the error,  $de(t)/dt$ , is calculated with backward differentiation and low-pass filtered by a first-order filter with a time constant,  $T_f$ , to avoid transient peaks in the derivative:

$$\frac{de(t_n)}{dt} = \frac{de(t_{n-1})}{dt} \frac{T_f}{\Delta t + T_f} + \frac{\Delta t}{\Delta t + T_f} \cdot \frac{e(t_n) - e(t_{n-1})}{\Delta t}. \quad (\text{A12})$$

Controller gains, derivative time filter constants, and neural delays utilized for the AHBM (Papers V and VI) studies are tabulated in Table A1. The time step,  $\Delta t$ , of the THUMS v3.0 is fixed to  $6.6 \cdot 10^{-7}$  s by mass scaling by using the keyword \*CONTROL\_TIMESTEP [10].

**Table A1. Controller gains, derivative filter time constants, neural delays, and activation dynamic time constants used for the validated AHBM (Paper V and VI).**

<b>Controller</b>	$k_p$	$k_i$	$k_d$	$T_f$	$T_{de}$	$T_{ne}$	$T_{naa}$	$T_{nad}$
Unit	<u>Contraction</u> rad	<u>Contraction</u> rad·s	<u>Contraction·s</u> rad	s	s	s	s	s
Head	0.865	1.263	0.578	0.0050	0.020	0.035	0.010	0.040
Cervical	1.301	1.476	0.467	0.0050	0.020	0.035	0.010	0.040
Lumbar	1.120	0.000	0.159	0.0050	0.025	0.035	0.010	0.040
Shoulder	1.059	1.000	0.437	0.0044	0.030	0.035	0.005	0.035
Elbow	2.000	1.000	0.062	0.0044	0.034	0.035	0.005	0.035

#### A.4 Muscle Recruitment and Activation Dynamics

A muscle recruitment strategy is used in which the AHBM muscle elements are grouped as either flexors or extensors for each controller. As the flexor and extensor groups have different maximum isometric strengths, the request to the muscle groups are scaled with the factors in Table A2, to provide a symmetrical controller response. The controller gains reported in Paper V are the product of the gains in the input keywords, Table A1, and the strength of the weakest muscle group for each controller in Table A2.

**Table A2. Strength of the flexor and extensor muscle groups in the AHBM, scale factors for the different muscle groups, and effective controller gains (Paper V). The muscles are grouped according to Table A3.**

<b>Muscle group</b>	<b>Head</b>	<b>Cervical</b>	<b>Lumbar</b>	<b>Shoulder</b>	<b>Elbow</b>
Flexors (Nm)	6.6	9.2	78.7	50.8	86
Extensors (Nm)	20.9	34.1	133.7	72.7	48.2
<b>Scale factor</b>					
Flexors	1	1	1	-1	0.578
Extensors	-0.317	-0.271	-0.588	0.698	-1
<b>Gains (Paper V)</b>					
$k_p$ (Nm/rad)	6	12	88	54	97
$k_i$ (Nm/rad·s)	8	14	0	51	48
$k_d$ (Nm·s/rad)	4	4	12	22	3

The scaled controller requests to each muscle group can be either positive or negative, but only positive scaled requests  $u_s(t)$  are passed through to the activation dynamics model. If the scaled request is negative, it is replaced by a zero request. The activation dynamics model is defined by two first order low pass filters in series [17] that generate muscle activation levels  $N_a(t)$ :

$$T_{ne} \frac{dN_e}{dt} = u_s(t) - N_e(t), \quad (\text{A13})$$

$$T_{na} \frac{dN_a}{dt} = N_e(t) - N_a(t). \quad (\text{A14})$$

The first filter is for an intermediate neural excitation level  $N_e(t)$ , driven by the absolute value of the scaled  $u_s(t)$ , one for each muscle group. The second filter for the activation level  $N_a(t)$  represents the contraction dynamics of the muscle; it is mainly dependent on the calcium ion release from the sarcoplasmic reticulum, which is rate limiting for the muscle contraction [18]. Muscle activation, the calcium release, is faster than deactivation, the calcium absorption, which is why the time constants,  $T_{na}$ , governing the contraction dynamics are split into two,  $T_{naa}$  for activation and  $T_{nad}$  for deactivation. The activation dynamics time constants are tabulated in Table A1. Furthermore, the excitation level,  $N_e(t)$ , and activation level,  $N_a(t)$ , are saturated at a maximum equal to one.

## A.5 Muscles Included

The Hill-model parameters for the muscles implemented in the AHBM (Paper I–II and V–VI), are tabulated in Table A3.

**Table A3. All muscles implemented in the AHBM. For all muscles the parameter  $PE_{max}$  is 0.8. No. = Number of elements; Func. = Function; A. tub. = Anterior tubercle; M. = Medial; P. tub. = Posterior tubercle; S. A. proc. = Superior articular process; T. proc. = Transverse process; HF = Head flexor; HE = Head extensor; CF = Cervical flexor; CE = Cervical extensor; LF = Lumbar flexor; LE = Lumbar extensor; SF = Shoulder flexor; SE = Shoulder extensor; EF = Elbow Flexor; EE = Elbow extensor; HiF = Hip flexor; HiE = Hip extensors; KF = Knee flexor; KE = Knee extensor; DF = Dorsiflexor; PF = Plantarflexor. \* Estimated; \*\* Moved from anatomical origin which is 1st–11th rib [4]; \*\*\* Only clavicular part of pectoralis major included in model.**

Muscle	No.	Func.	Origin	Insertion	PSCA [mm <sup>2</sup> ]	$\sigma_{max}$ [MPa]	sno [-]	C <sub>sh</sub> [-]	srm [-]	C <sub>short</sub> [-]	C <sub>leng</sub> [-]	C <sub>mvl</sub> [-]	C <sub>pe</sub> [-]
Erector spinae longissimus cervicis	5	CE	T. proc. C2–C6 [14]	T. proc. T2–T6	149 [16]	0.5	0.9	0.5	2.2	0.25	0.1	1.5	6.0
Erector spinae iliocostalis cervicis	3	CE	P. tub. C4–C6 [12]	4 <sup>th</sup> –6 <sup>th</sup> rib	99 [16]	0.5	0.9	0.5	2.2	0.25	0.1	1.5	6.0
Multifidus cervicis	12	CE	S. proc. C2–C7 [12][1]	T. proc. C5–T4	450 [15]	0.5	0.9	0.5	2.2	0.25	0.1	1.5	6.0
Semispinalis cervicis	4	CE	S. proc. C2–C5 [12]	T. proc. T1–T4	310 [16]	0.5	0.9	0.5	2.2	0.25	0.1	1.5	6.0
Semispinalis thoracis	2	CE	S. proc. C6–C7 [12]	T. proc. T5–T6	140*	0.5	0.9	0.5	2.2	0.25	0.1	1.5	6.0
Splenius cervicis	3	CE	T. proc. C1–C3 [12]	S. proc. T3–T5	144 [16]	0.5	0.9	0.5	2.2	0.25	0.1	1.5	6.0
Levator scapulae	4	CE	T. proc. C1–C4 [12]	Scapula	312 [16]	0.5	0.9	0.5	2.2	0.25	0.1	1.5	6.0
Obliquus capitis inferior	1	CE	T. proc. C1 [12]	S. proc. C2	195 [16]	0.5	0.9	0.5	2.2	0.25	0.1	1.5	6.0
Scalenus posterior	3	CF	T. proc. C4–C6 [14][12]	1 <sup>st</sup> rib	105 [16]	0.5	0.9	0.5	2.2	0.25	0.1	1.5	6.0
Scalenus medius	6	CF	C2–C7 [12]	1 <sup>st</sup> rib	138 [16]	0.5	0.9	0.5	2.2	0.25	0.1	1.5	6.0
Scalenus anterior	4	CF	A. tub. C3–C6 [14]	1 <sup>st</sup> rib	188 [16]	0.5	0.9	0.5	2.2	0.25	0.1	1.5	6.0
Longus colli superior oblique	3	CF	Anterior arch C1 [12]	T. proc. C3–C5	81 [8]	0.5	0.9	0.5	2.2	0.25	0.1	1.5	6.0
Longus colli vertical	4	CF	Vertebral body C2–C4 [12]	Vertebral body C7–T3	90 [8]	0.5	0.9	0.5	2.2	0.25	0.1	1.5	6.0
Longus colli inferior oblique	2	CF	T. proc. C5–C6 [12]	Vertebral body T1–T2	40 [8]	0.5	0.9	0.5	2.2	0.25	0.1	1.5	6.0
Tibialis anterior	1	DF	Proximal, lateral side of tibia [12]	Medial cuneiform	1100 [2]	0.5	0.95	0.33	5.0	0.3	0.005	1.35	6.95

Triceps, element 1	1	EE	Scapula [12]	Olecranon process	570 [9]	1.0	0.98	0.64	5.0	0.3	0.005	1.25	3.0
Triceps, element 2	1	EE	Humerus [12]	Olecranon proc.	450 [9]	1.0	0.97	0.48	5.0	0.3	0.005	1.25	3.0
Triceps, element 3	1	EE	Humerus [12]	Olecranon proc.	150 [9]	1.0	0.95	0.64	5.0	0.3	0.005	1.25	3.0
Triceps, element 4	1	EE	Humerus [12]	Olecranon proc.	150 [9]	1.0	0.90	0.87	5.0	0.3	0.005	1.25	3.0
Triceps, element 5	1	EE	Humerus [12]	Olecranon proc.	150 [9]	1.0	0.90	1.34	5.0	0.3	0.005	1.25	3.0
Biceps brachii, long head	1	EF	Glenohumeral joint [12]	Radial tuberosity	450 [9]	1.0	1.034	0.14	5.0	0.3	0.005	1.35	6.15
Biceps brachii, short head	1	EF	Coracoid proc. [12]	Radial tuberosity	310 [9]	1.0	1.033	0.21	5.0	0.3	0.005	1.35	6.15
Brachialis, element 1	1	EF	Humerus [12]	Ulnar tuberosity	355 [9]	1.0	1.06	0.50	5.0	0.3	0.005	1.35	6.15
Brachialis, element 2	1	EF	Humerus [12]	Ulnar tuberosity	355 [9]	1.0	1.073	0.60	5.0	0.3	0.005	1.35	6.15
Brachioradialis	1	EF	Humerus [12]	Radius, distal end	190 [9]	1.0	1.0	0.14	5.0	0.3	0.005	1.35	6.15
Pronator teres	1	EF	M. epicondyle of humerus [12]	Radius, medial end	400 [9]	1.0	1.038	0.35	5.0	0.3	0.005	1.35	6.15
Extensor carpi radialis longus	1	EF	Humerus [12]	Second metacarpal	220 [9]	1.0	1.01	0.35	5.0	0.3	0.005	1.35	6.15
Erector spinae longissimus capitis	8	HE	Mastoid process [14]	T. proc. C4–T4	98 [16]	0.5	0.9	0.5	2.2	0.25	0.1	1.5	6.0
Semispinalis capitis	5	HE	Occipital bone [15][14]	S.A. proc. C4–C7 T. proc. T3	550 [16]	0.5	0.9	0.5	2.2	0.25	0.1	1.5	6.0
Splenius capitis	6	HE	Mastoid process [12]	S. proc. C5–T3	312 [16]	0.5	0.9	0.5	2.2	0.25	0.1	1.5	6.0
Trapezius	3	HE	Skull [16]	Clavicula	378 [16]	0.5	0.9	0.5	2.2	0.25	0.1	1.5	6.0
Rectus capitis posterior minor	1	HE	Occipital bone [12]	P. tub. C1	92 [16]	0.5	0.9	0.5	2.2	0.25	0.1	1.5	6.0
Rectus capitis posterior major	1	HE	Occipital bone [12]	Spine of C2	168 [16]	0.5	0.9	0.5	2.2	0.25	0.1	1.5	6.0
Rectus capitis lateralis	1	HE	Skull [12]	C1	70 [8]	0.5	0.9	0.5	2.2	0.25	0.1	1.5	6.0

Obliquus capitis superior	1	HE	Occipital bone [12]	T. proc. C1	88 [16]	0.5	0.9	0.5	2.2	0.25	0.1	1.5	6.0
Rectus capitis anterior	1	HF	Skull [12]	C1	70 [8]	0.5	0.9	0.5	2.2	0.25	0.1	1.5	6.0
Longus capitis	4	HF	Occipital bone [14][12]	T. proc. C3–C6	136 [16]	0.5	0.9	0.5	2.2	0.25	0.1	1.5	6.0
Sternocleidomastoid	2	HF	Mastoid process [14][12]	Clavicula and sternum	492 [16]	0.5	0.9	0.5	2.2	0.25	0.1	1.5	6.0
Adductor magnus	4	HiE	Inferior ramus of pubis [12]	Linea aspera, along femur	2130 [2]	0.5	1.23–1.45	0.25–0.6	5.0	0.3	0.005	1.35	6.95
Gluteus maximus	3	HiE	Iliac crest and coccyx [12]	Gluteal tuberosity on femur	3040 [2]	0.5	1.45–1.80	0.6–1.1	5.0	0.3	0.005	1.25	6.95
Biceps femoris	2	HiE, KF	Ischial tuberosity and linea aspera, mid femur [12]	Lateral condyle of tibia	1680 [2]	0.5	0.9–0.95	0.2–0.3	5.0	0.3	0.005	1.35	6.95
Semi-membranosus	1	HiE, KF	Ischial tuberosity [12]	Medial tibial condyle	1910 [2]	0.5	0.92	0.2	5.0	0.3	0.005	1.35	6.95
Semitendinosus	1	HiE, KF	Ischial tuberosity [12]	Proximal, medial surface of tibia	490 [2]	0.5	0.92	0.2	5.0	0.3	0.005	1.35	6.95
Adductor longus	1	HiF	Front of pubis [12]	Linea aspera, mid femur	650 [2]	0.5	0.9	0.25	5.0	0.3	0.005	1.35	6.95
Iliacus	1	HiF	Iliac fossa [12]	Lesser trochanter	1020 [2]	0.5	0.9	0.25	5.0	0.3	0.005	1.35	6.95
Pectineus	1	HiF	Pectineal line [12]	Linea aspera, proximal end	290 [2]	0.5	0.8	0.33	5.0	0.3	0.005	1.35	6.95
Psoas	1	HiF	L2 vertebra [12]	Lesser trochanter	790 [2]	0.5	0.9	0.25	5.0	0.3	0.005	1.35	6.95
Rectus femoris	1	HiF, KE	Anterior inferior iliac spine [12]	Quadriceps tendon	1390 [2]	0.5	1.0	0.8	5.0	0.3	0.005	1.35	6.95
Sartorius	1	HiF, KF	Anterior superior iliac spine [12]	Proximal, medial surface of tibia	190 [2]	0.5	0.9	0.25	5.0	0.3	0.005	1.35	6.95
Vastus	3	KE	Anterior, upper third of femur [12]	Quadriceps tendon	7750 [2]	0.5	1.0	0.8	5.0	0.3	0.005	1.25	6.95

Gastrocnemius	2	KF, PF	Medial and lateral condyles of femur [12]	Calcaneal tuberosity	3130 [2]	0.5	0.95	0.33	5.0	0.3	0.005	1.35	6.95
Quadratus lumborum	5	LE	12 <sup>th</sup> rib, T. proc. L1–L4 [3]	Iliac crest	280 [6]	0.5	0.9	0.5	2.2	0.25	0.1	1.5	6.0
Multifidus thoracis	8	LE	S. proc. T8–12 [12]	T. proc. L1– L4	464 [5]	0.5	0.9	0.5	2.2	0.25	0.1	1.5	6.0
Multifidus lumborum	13	LE	S. proc. L1–L5 [3]	L4–L5, Sacrum, Iliac crest	833 [4]	0.5	0.9	0.5	2.2	0.25	0.1	1.5	6.0
Erector spinae longissimus thoracis pars thoracis	12	LE	7 <sup>th</sup> –12 <sup>th</sup> rib**	S. proc. L2– L5, Sacrum	1109 [4]	0.5	0.9	0.5	2.2	0.25	0.1	1.5	6.0
Erector spinae longissimus thoracis pars lumborum	5	LE	T. proc. L1–L5 [4]	Iliac crest	499 [4]	0.5	0.9	0.5	2.2	0.25	0.1	1.5	6.0
Erector spinae iliocostalis lumborum pars thoracis	8	LE	12 <sup>th</sup> rib**	Iliac crest	547 [4]	0.5	0.9	0.5	2.2	0.25	0.1	1.5	6.0
Erector spinae iliocostalis lumborum pars lumborum	4	LE	T. proc. L1–L4 [4]	Iliac crest	633 [4]	0.5	0.9	0.5	2.2	0.25	0.1	1.5	6.0
Rectus abdominis	3	LF	5 <sup>th</sup> –7 <sup>th</sup> costal cartilage [13][12]	Crest of pubis	567 [13]	0.5	0.98	0.5	2.2	0.25	0.1	1.5	7.2
Internal oblique	2	LF	Costal cartilage[13][12]	Iliac crest	710 [13]	0.5	0.9	0.5	2.2	0.25	0.1	1.5	7.2
External oblique	2	LF	Costal cartilage[13][12]	Iliac crest	905 [13]	0.5	0.9	0.5	2.2	0.25	0.1	1.5	7.2
Teres major	1	SE	Inferior angle of scapula [12]	Humerus	300 [9]	1.0	0.95	0.50	5.0	0.3	0.005	1.35	6.15
Latissimus dorsi	3	SE	Spinous process of T12, L3, and L5 [12]	Humerus	760 [9]	1.0	0.95	0.50	10.0	0.3	0.005	1.35	6.15
Deltoid, posterior	3	SE	Acromion and scapular ridge [12]	Humerus	190 [9]	1.0	0.95	0.50	10.0	0.3	0.005	1.35	6.15

Deltoid, anterior	1	SF	Lateral third of clavicle [12]	Humerus	820 [9]	1.0	0.95	0.50	10.0	0.3	0.005	1.35	6.15
Deltoid, middle	1	SF	Lateral margin of the acromion [12]	Humerus	820 [9]	1.0	0.95	0.50	10.0	0.3	0.005	1.35	6.15
Pectoralis major***	1	SF	Sternal half of clavicle [12]	Humerus	260 [9]	1.0	0.95	0.50	5.0	0.3	0.005	1.35	6.15
Coracobrachialis	1	SF	Coracoid process [12]	Humerus	170 [9]	1.0	0.95	0.50	5.0	0.3	0.005	1.35	6.15

## A.6 References

- [1] Anderson JS, Hsu AW, Vasavada AN (2005) Morphology, Architecture, and Biomechanics of Human Cervical Multifidus. *Spine* 30:E86–91.
- [2] Arnold EM, Ward SR, Lieber RL, Delp SL (2010) A Model of the Lower Limb for Analysis of Human Movement. *Annals of Biomedical Engineering* 38(2):269–279.
- [3] Bogduk N, Endres SM (2005) *Clinical Anatomy of the Lumbar Spine and Sacrum*. Elsevier Churchill Livingstone, London, UK.
- [4] Bogduk N, Macintosh JE, Percy MJ (1992) A Universal Model of the Lumbar Back Muscles in the Upright Position. *Spine* 17:897–913.
- [5] Daggfelt K, Thorstensson A (2003) The Mechanics of Back-extensor Torque Production about the Lumbar Spine. *Journal of Biomechanics* 36:815–825.
- [6] Delp SL, Suryanarayanan S, Murray WM, Uhlir J, Triolo RJ (2001) Architecture of the Rectus Abdominis, Quadratus Lumborum, and Erector Spinae. *Journal of Biomechanics* 34:371–375.
- [7] Erhart T (2010) An Overview of User Defined Interfaces in LS-DYNA. Paper presented at the LS-DYNA Forum; Bamberg, Germany.
- [8] Hedenstierna S (2008) *3D Finite Element Modeling of Cervical Musculature and its Effect on Neck Injury Prevention*. Ph.D. Thesis; Royal Institute of Technology, Stockholm, Sweden.
- [9] Holzbaur KRS, Murray WM, Delp SL (2005) A Model of the Upper Extremity for Simulating Musculoskeletal Surgery and Analyzing Neuromuscular Control. *Annals of Biomedical Engineering* 33:829–840.
- [10] LSTC (2013) *LS-DYNA User's Manual Volume I, Version 971 R6.1.0*. Livermore Software Technology, Livermore, CA, USA.
- [11] LSTC (2013) *LS-DYNA User's Manual Volume II: Material Models, Version 971 R6.1.0*. Livermore Software Technology, Livermore, CA, USA.
- [12] Standring S (ed.) (2008) *Gray's Anatomy – The Anatomical Basis of Clinical Practice*. Elsevier Churchill Livingstone, London, UK.
- [13] Stokes IAF, Gardner–Morse M (1999) Quantitative Anatomy of the Lumbar Musculature. *Journal of Biomechanics* 32:311–316.
- [14] Toyota (2008) *Users' Guide of Computational Human Model THUMS® – AM50 Occupant Model: Version 3.0–080225*. Toyota Motor Corporation, Toyota Central Labs Inc, Toyota City, Aichi, Japan.
- [15] van der Horst M (2002) *Human Head Neck Response in Frontal, Lateral and Rear End Impact Loading – Modeling and Validation*. Ph.D. Thesis; Eindhoven University of Technology, Eindhoven, the Netherlands.
- [16] Van Ee CA, Nightingale RW, Camacho DLA, Chancey VC, Knaub KE, Sun EA, Myers BS (2000) Tensile properties of the Human Muscular and Ligamentous Cervical Spine. *Stapp Car Crash Journal* 44:85–102.
- [17] Winters JM, Stark L (1985) Analysis of Fundamental Human Movement Patterns through the Use of In-depth Antagonistic Muscle Models. *IEEE Transactions on Biomedical Engineering* 32(10):826–839.

- [18] Winters JM, Stark L (1987) Muscle Models: What is Gained and What is Lost by Varying Muscle Model Complexity. *Biological Cybernetics* 55:403–420.
- [19] Wittek A, Kajzer J (1997) Modeling the Muscle Influence on the Kinematics of the Head-Neck Complex in Impacts. *Memoirs of the School of Engineering Nagoya University* 49:155–205.